# A New Haze Removal Algorithm for Single Urban Remote Sensing Image

**SHIQI HUANG**[1], (Member, IEEE), **YANG LIU**[1], **YITING WANG**[2], **ZULIANG WANG**[3], **AND JINKU GUO**[4,5]

[1]School of Automation, Xi'an University of Posts & Telecommunications, Xi'an 710121, China
[2]Rocket Force University of Engineering, Xi'an 710025, China
[3]Xijing University, Xi'an 710123, China
[4]Unmanned System Research Institute, Northwestern Polytechnical University, Xi'an 710068, China
[5]Xian Daheng Tian Cheng IT Company, Ltd., Xi'an 710026, China

Corresponding author: Shiqi Huang (greatsar602@163.com)

**ABSTRACT** The remote sensing imaging detection technology is an important means to effectively monitor and manage urban environment and resources, and remote sensing images are an important data source of smart city and digital city. The existence of haze has a serious impact on the quality of optical remote sensing image acquisition, resulting in remote sensing image blurred, detail information loss, contrast decreased and color distortion. To reduce the impact of haze and give full play to the value of remote sensing images, a new urban remote sensing haze removal (URSHR) algorithm is proposed in this paper, which combines the image phase consistency feature, multi-scale Retinax theory and histogram characteristic. In URSHR method, firstly the image haze is removed by using multi-scale Retinex theory and histogram characteristic, and then the detail information of the image is enhanced by using the phase consistency features, finally they are fused with the multi-scale wavelet transform. It achieves the purpose of both removing haze and enhancing geometric detail information. The many verification experiments were carried out by using real urban remote sensing image data, and good results were obtained. This shows that the new algorithm is a feasible and effective for urban remote sensing image haze removal, and it has good application and promotion value.

**INDEX TERMS** Urban remote sensing image, phase consistency, haze removal, multi-scale analysis, Retinex theory, histogram characteristic.

## I. INTRODUCTION

Haze has become a common severe weather phenomenon, which brings great challenges and difficulties to outdoor monitoring and remote sensing detection system. When the haze weather occurs, there are a lot of suspended particles in the air, such as water droplets and aerosols, which have strong scattering and absorption effect on the light, so that the light will produce strong attenuation in the process of propagation. The attenuation of light intensity will lead to the degradation of image quality, like reduced clarity, blurred details and color distortion. This brings great difficulties to image processing, interpretation and application. At the same time, it seriously

The associate editor coordinating the review of this manuscript and approving it for publication was Yudong Zhang.

affects the normal work of various optical imaging instrument systems, such as outdoor monitoring system, aerospace and aviation remote sensing system, target tracking and recognition system. Therefore, haze removal is an important part of remote sensing image preprocessing.

The image haze removal came from the outdoor image processing. At present, many effective theories and methods have been developed [1]–[10]. These methods can be divided into four types. The first type is the image enhancement processing based on filters [1], [2], [7]–[9], [11], such as the histogram equalization [7,11], the Retinax theory [1], [2] and the bilateral filter [12]. The second type is the image restoration processing based on the atmospheric physical model [3]–[6], and the typical method is the dark channel prior (DCP) method [3]. The third type is the fusion methods

based on a single method or feature [9], [13], [14]. The fourth type is the network models based on various machine learning [10], [15]–[18].

When the light passes through the atmosphere in haze weather, the water droplets or particles will mask and reflect the passing light, which not only reduces the visibility and contrast [19], but also makes the obtained image blurred. Therefore, the first strategy that scholars think of is to filter out haze to achieve the purpose of enhancing the image. The histogram processing is a classic method to stretch the gray value range of an image. Although it is easy to operate and can obtain good effect of removing haze, it is also easy to cause the detail information lost and to produce the phenomenon of over enhancement and color distortion. To solve the problem of blurred details, some improved local equalization algorithms were proposed [11], [20]. They divide the image into several regions, then carry out histogram equalization for each region, and finally overlay the processed results of all local regions, so as to achieve the purpose of removing haze and enhancing detail information. Obviously, the computation of a local algorithm is increased significantly, and the enhancement effect is not obvious when the difference between foreground and background gray is small. To suppress over enhancement and color distortion, some improved algorithms based on image brightness preservation were proposed, for example, the brightness preserving bi-histogram equalization (BBHE) [21], dynamic histogram equalization (DHE) [22], and brightness protection dynamic histogram equalization (BPDHE) [7]. Combined with fuzzy theory, a brightness protection dynamic fuzzy histogram equalization (BPDFHE) algorithm was proposed based on BPDHE algorithm in [8]. They can keep the brightness of the original image well and reduce the color distortion, but the effect of image haze removal is not significant. The Retinex algorithm based on the theory of retina and cerebral cortex is a very excellent method in image haze removal and enhancement [23]–[25]. The Retinex theory assumes that light changes slowly and object reflects violently, through filtering out light components and retaining reflection components, and the result is that a haze-free image is obtained. Because the Retinex theory can highlight the edge details of the image, it is widely used in image haze removal field. Jobson proposed a single-scale Retinex (SSR) algorithm based on the central surround function [26], [27]. The SSR algorithm can enhance the image by setting a Gaussian scale parameter constant, but different scale parameter values will bring great impact on the image processing effect. If the value is not appropriate, it will lead to poor haze removal effect and color distortion. Therefore, for different haze images, the robustness and universality of the algorithm are poor. Aiming at the shortcomings of SSR algorithm, an improved multi-scale Retinex (MSR) algorithm was proposed [1]. To enhance the generalization ability for different images, the MSR algorithm uses multiple Gaussian scale parameters to process an image and perform weighted average. No matter SSR or MSR algorithm, at the edge where

the color or brightness of the image varies greatly, it is easy to cause image halo. Therefore, some scholars proposed the Retinex algorithm of color recovery type [28], [29]. On the whole, the Retinex theory can well remove haze in the image. However, the processed results are a little darker in color, and it is also difficult to enhance the detail information in the brighter part of the haze image.

Using the filtering theory of image enhancement to remove haze does not consider the reason of haze image quality reduction, and the essence of image eliminating haze is to restore the image that is not affected by haze, i.e. haze-free image. Therefore, haze removal based on the physical model of atmospheric scattering is an important strategy for image restoration. Tan *et al.* used the physical scattering model of atmosphere to remove haze in a single image [5]. It is based on two assumptions. One is that the contrast of natural clear image in sunny days is higher than that in haze. Another is that the amount of ambient light depends on the depth of the object in the image. Using the Markov random field, [5] can recover the edge information of the image and obtain the image with improved contrast. At the same time, it is easy to make the contrast of the image tend to over compensate, resulting in color distortion and halo effect at the sudden change of depth of field. Based on the assumption that the transmitted light is independent of the color of the object's surface, Fattal proposed an algorithm to estimate the transmission by using independent components analysis [6], and further recovered the haze-free image by adopting the atmospheric scattering model. Since the algorithm relies on local hypothesis statistics, it is not only computationally expensive, but also ineffective in dense haze area. At the same time, it is based on the statistical characteristics of color image, so the algorithm cannot process gray images. He *et al.* proposed a dark channel priori (DCP) method by observing a large number of outdoor images [3]. The DCP algorithm is one of the most effective methods in the field of image dehazing, which can restore the clear image without haze. However, when most areas of the target scene do not satisfy the dark channel prior, such as large gray-attribute areas, white objects and sky areas, or it is a gray image, the DCP algorithm often fails. Due to the use of soft matting algorithm, when the image scale is large, the DCP algorithm not only has a large amount of computation, but also has a long operation time, so its real-time performance is poor. Aiming at the defect of the DCP method, many researchers put forward some corresponding improved algorithms [30]–[32]. These methods are based on the physical model of atmospheric scattering; generally, they cannot obtain good results until the assumptions are valid. In addition, it is necessary to estimate the parameters of ambient atmospheric light amount and atmospheric transmittance. The accuracy of parameter estimation directly affects the haze removal effect. To improve haze removal effect, there were many methods proposed for the two parameters estimation [33]–[35].

It is known from above analysis that each method has its advantage and limitation. The basic reason is that some

methods are put forward to deal with specific haze images and special purposes. When other images are used for substitution processing, the effect will be different. To improve the generalization ability or robustness of an algorithm, some scholars proposed that different methods or features are fused to achieve the haze removal [9], [14], [36]–[39]. Using fusion strategy to process images, the key technology is how to determine the fusion rule, because different rules will produce different results. In recent years, the deep learning theory represented by the convolution neural network (CNN) has achieved good success in image classification and target detection. Therefore, some scholars try to use the deep learning theory to solve the problem of haze removal in images [10], [15], [17], [40]–[42]. The biggest difficulty of haze removal of single image based on deep learning is the acquisition and training of image samples. Since a large number of training sample feature sub-image sets need be generated [43], the whole process is relatively complex, the speed is slow, and the real-time performance is poor.

The haze removal of remote sensing images is not only challenging, but also of great application value, which has been gradually attracted by a lot of scholars [9], [44], [45]. There are many image haze removal algorithms, and all of them can achieve good results, but the processed objects are usually outdoor color images or RGB images. If one directly uses these methods to process remote sensing image, he cannot get satisfactory results. There are great differences between remote sensing images and common outdoor color images. First, there is very large difference in resolution. The resolution of remote sensing images is low, but that of outdoor images is high. Second, outdoor images are color images, while remote sensing images include gray, color or multispectral images. Third, some outdoor images contain sky background, the depth of field is longer, and the scene span is larger, so the focus of outdoor image processing is the distant view part. Fourth, the remote sensing image contains the gray distribution of the earth's surface scene, and the depth of field is relatively small. Although haze can affect the quality and definition of an image, it cannot change the gray level and spatial distribution of objects in remote sensing images. In other words, whether there is haze or not, whether it affects the remote sensing image or not, the phase information of the object in the remote sensing image is unchanged, because their spatial distribution is constant. Therefore, this paper uses the phase information of remote sensing image and Retinex theory to remove the haze of urban remote sensing image. It can not only effectively remove the haze in the urban remote sensing image, but also maintain the rich information and more complete details, which is more close to the original scene. The main contribution of this paper is to propose a new urban remote sensing haze removal (URSHR) algorithm, which combines the phase information, statistical characteristics and multi-scale Retinex theory. Experimental results show that the new method can effectively remove the haze, the effect is very good, and can obtain accurate details. Urban remote sensing is an important branch of remote sensing technology and is also an important data source of smart city and digital city, so the method proposed in this paper has important theoretical significance and promotion value for urban remote sensing image processing.

The URSHR algorithm has some following advantages. (1) It can process panchromatic image, multispectral single band gray image, multispectral color image and RGB image, and has strong universality. (2) Using the cascade processing of multi-scale Retinex theory and histogram characteristics, the haze of remote sensing image can be effectively removed. (3) The edges of the remote sensing image are enhanced by using the phase consistency features, and the clearer details are got. (4) Using wavelet multi-scale decomposition theory to perform the fusion operation, the recovered information is more accurate and complete. In addition, for some special field images, such as outdoor images with sky area or remote sensing images with a large area of forest and a large wave ocean, the processing effect may not be ideal, because they produce too many complex dynamic details and beyond the scope of the URSHR algorithm. The URSHR algorithm is proposed for urban remote sensing images, so it can achieve good results and performance even for remote sensing images including large areas of green grassland, trees, rivers, lakes, pools and parks.

The rest of this paper is organized as follows. In section II, the remote sensing image characteristics and preliminary work are briefly introduced. The proposed URSHR algorithm is described in detail in section III. In section IV, the experimental settings and the results are discussed, including different methods and images. Finally, section V concludes this paper and mentions the future work.

## II. RELATED WORK

The broad remote sensing imaging technology refers to the technology that can acquire the electromagnetic information of a target but without touching it. According to this definition, remote sensing images include these obtained from traditional platforms, such as aircrafts and satellites, and those obtained by ordinary cameras, mobile phones and video cameras. Therefore, remote sensing has entered the era of big data of multi-source remote sensing. The narrow definition of remote sensing refers to the technology of collecting the electromagnetic radiation information of the earth's surface target from the satellites, aircrafts or planes, and identifying the earth's environment and resources. Here, the remote sensing images refer to the ground surface images obtained from high-altitude platforms like satellites, planes or unmanned aerial vehicle (UAV), excluding various outdoor images obtained from the ground platform. The remote sensing image is not only different from outdoor images, but also has its own unique characteristics. In this paper, the characteristics and imaging mechanism of remote sensing image are studied in detail as follows.

(1) Remote sensing image is a low resolution image. Its spatial resolution is relatively low, which is often described in meters. At present, the open commercial remote sensing

image has the highest spatial resolution of 0.31m. But the spatial resolution of outdoor images is very high, as is described in pixels.

(2) The scene span of remote sensing image is small. The remote sensing image is acquired from the air. If the imaging sensor is vertical to the ground, the scene transmission is very little difference. Therefore, the influence of haze on the scenery is almost the same. For outdoor images, especially those with sky background, the depth of field is very long, and the degree of influence by haze is quite different.

(3) A remote sensing image is a large-scale regional imaging. The lower the resolution is, the larger the area is. A remote sensing image usually covers a large area of scene, which can reach thousands of square kilometers. However, the field of view of the outdoor image is very limited.

(4) Remote sensing imaging technology obtains the information of looking down. It observes the earth's surface from the space, and gets the looking down information. Outdoor images usually get parallel information obtained from the ground, i.e. the information of one side of the object.

(5) The remote sensing image has no sky background. Most of the outdoor images contain the sky background area, and the remote sensing image does not contain the sky area.

(6) There are various types of remote sensing images. Now the outdoor images are RGB color images. Remote sensing images not only include the single band gray images and panchromatic images, but also multispectral color images synthesized by multiple bands or RGB images obtained directly by camera sensors.

(7) The feature clarity obtained from remote sensing image is relatively stable. In the outdoor images, the details of the near scene are relatively clear, and the details of the far scene are generally vague, so the focus of processing is on the far scene part. The detail clarity of the whole region of the remote sensing image is almost same.

(8) The urban remote sensing image includes rich detail information. Urban remote sensing image contains almost artificial buildings, with rich details and clear outlines, and the abrupt changes of edge information are more intense. The walls and roofs of most buildings are gray, white or red.

(9) An urban remote sensing image contains a variety of ground objects. There are usually green grass, green trees, pools, rivers, lakes, houses, campus, stadium, parks, squares and vehicles. Outdoor images contain relatively simple types of ground objects.

Due to different acquisition platforms between outdoor images and remote sensing images, the image features or information obtained are also quite different. Although outdoor images have good haze removal algorithms, if they are directly used for removing haze of remote sensing images, the processing effect is not ideal, especially for urban remote sensing images. In remote sensing images, urban buildings are represented by gray or white roofs, walls and pavements, as well as other colors such as green, blue and red. The DCP algorithm proposed in [3] is a very effective haze removal algorithm as long as it satisfies the prior assumption, and

has been widely used. However, the DCP algorithm is not suitable for urban remote sensing image. Because there are many white or gray buildings in the urban remote sensing image, it does not meet the assumptions of the DCP algorithm, which affects the effect of haze removal. According to the characteristics of remote sensing image, the literature [9] proposed a haze removal algorithm based on the multi-scale model and histogram characteristics (MSMHC) for remote sensing images. In this algorithm, the selection of scale parameters and the range of application were discussed in detail. Therefore, the number and value of the corresponding scale parameters are directly set in the URSHR algorithm in this paper. Although the MSMHC algorithm can effectively reduce the impact of haze, maintain better details, and has better universality. But for the urban remote sensing images, its contrast and clarity still need to be improved. Especially in the edge of the house building or roofs, there is a large difference in color or brightness with other objects around, which easily leads to appear halo phenomenon with the MSMHC algorithm. This case can be seen in the experiments in Section IV.

Artificial buildings in remote sensing images, such as houses and streets, can maintain good phase consistency, and their existence and distribution will not be affected by haze and other factors. Using phase consistency can effectively improve the detail information of contrast, especially the artificial targets. Phase consistency (PC) is an important property of an image. Using the PC model, ones can well get the structural contour information of the object in the image, and it is not affected by the change of brightness and contrast of the image. In the process of studying the Mach band effect, Morrone *et al.* found a rule that the signal always appeared at the maximum superposition point in the Fourier phase, then they proposed the PC model [46]. The PC feature is a way to measure the phase similarity of each position and each frequency component of the image, which can well detect the edge and feature point information in the image. Therefore, some scholars use the PC model to complete the edge and crack detection [47]–[49]. Because the PC feature is not affected by haze, this paper proposed a new urban remote sensing image haze removal algorithm based on the phase consistency feature of remote sensing images and multi-scale statistical features, namely the URSHR algorithm, which will be introduced in detail in the next part.

## III. DESCRIPTION OF ALGORITHM PRINCIPLE AND IMPLEMENTATION PROCESS

The theories and methods of image haze removal are generally proposed for outdoor images. There are few algorithms involved in remote sensing image haze processing. In recent years, some scholars have began to pay attention to the problem [9], [43]–[45], [50], [51]. Although they deal with the haze problem in remote sensing image, the processing idea is basically the same as outdoor image. If one wants to get the ideal effect, he must combine the characteristics of remote sensing image, the advantages and disadvantages of
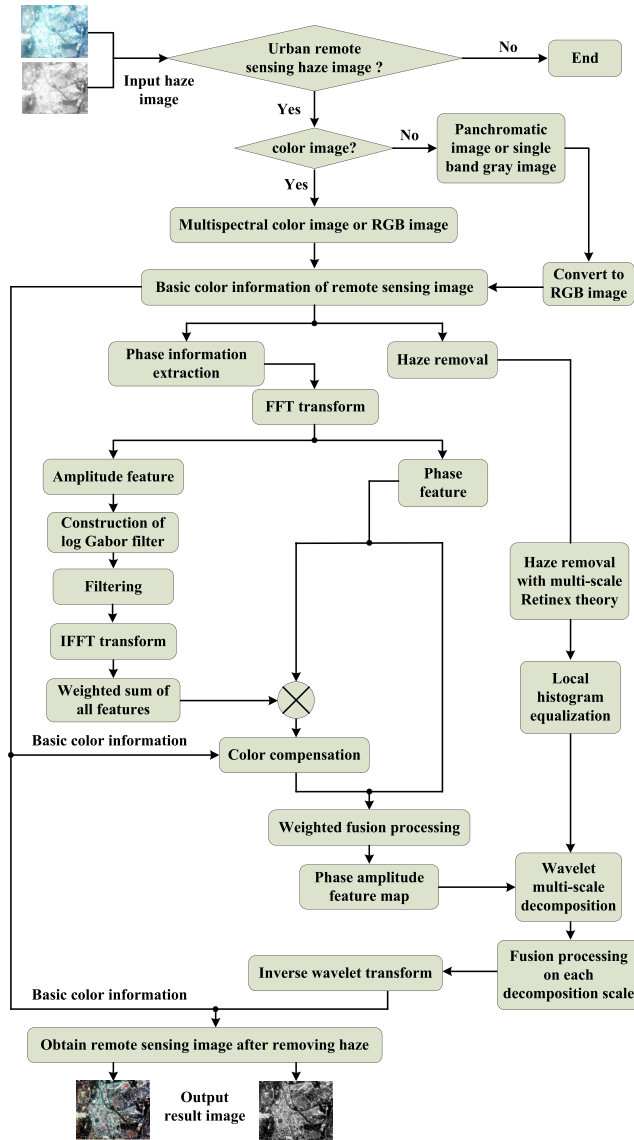
**FIGURE 1.** Schematic diagram of the URSHR algorithm.

the existing algorithm and the scope of its applications. Based on the characteristics and connotative information of urban remote sensing image, the URSHR algorithm was proposed in this paper. An urban remote sensing image contains a lot of artificial building edges, streets and roads information. The color of the wall or roof of the building is bright, the cross reflection light and the environment light are strong and complex. Therefore, it is not ideal to use the usual outdoor image processing method to remove the haze in urban remote sensing image. However, the haze removal algorithm, such as the URSHR algorithm, which is specially designed for the characteristics of urban remote sensing image, can achieve good results. The principle block diagram of the URSHR algorithm is shown in Fig.1. The main implementation steps of it are as follows.

(1) Input an image and judge whether it is an urban remote sensing image. Firstly, the input image is judged by vision, whether it is urban remote sensing image or not. If it is not,

the algorithm ends; if it is an urban remote sensing image, it goes to the next step. The input remote sensing image can be a panchromatic image, single band gray image, RGB or multispectral color image. These input optical remote sensing images have been affected by haze to varying degrees.

(2) Determine whether it is a color image. Here we mainly judge whether the input urban remote sensing image is a color image or a gray image, and save the relevant color information to provide information for subsequent color supplement operation and output results. If it is a gray image, it goes to the step three; if it is a color image, it directly goes to step four.

(3) A gray image is changed into a color image. To facilitate the same processing steps and processes as multi band color remote sensing images, the input gray image or panchromatic image performs the color enhancement processing. Suppose that the input single band gray remote sensing image is represented by $I(m, n)$, and the converted RGB false color remote sensing image is represented by $IC(m, n)$. The transformation process is shown in equation (1). Each pixel value of gray image $I(m, n)$ is assigned to three channels of false color RGB image $IC(m, n)$ at the same time, namely $IC_R(m, n)$, $IC_G(m, n)$ and $IC_B(m, n)$ channels.

$$\begin{cases} IC_R(m, n) = I(m, n) \\ IC_G(m, n) = I(m, n) \\ IC_B(m, n) = I(m, n) \end{cases} \tag{1}$$

Like the typical DCP algorithm, the required input image is not only a color image, but also the pixel values of the three channel images are not equal. This is the obvious deficiency of methods based on the atmospheric scattering model. The URSHR algorithm transforms a gray image into a color image by equation (1). It shows that the URSHR algorithm can not only process color multispectral image, but also process single band gray image, which shows that it has a wide range of application and better universality.

(4) The Fourier transform is performed on the input urban remote sensing image. The acquisition of phase information is completed in the frequency domain, so first of all it is to transform the original image from the spatial domain to the frequency domain. Its purpose is to extract phase information and phase consistency features of an image.

(5) Obtain the phase consistency feature map. Phase consistency feature is an important content and connotation of urban remote sensing images. It contains very rich and significant edge and contour information. It is very important for the detection of urban buildings, roads and other urban targets. The extraction process of image phase consistency features, please refer to relevant references [52]–[54]. The phase consistency feature will be used for convolution and fusion with the amplitude feature.

The PC model is a measure of the phase similarity of each position and frequency component of an image. It can obtain reliable image contour information without the influence of image brightness and contrast. To process image

conveniently and to extract two-dimensional phase information of an image, the phase consistency definition of two-dimensional space is given in equation (2) [53].

$$PC(x) = \frac{\sum_n W(x)|E_n(x) - T|}{\sum_n A_n(x) + \varepsilon} \qquad (2)$$

Here $A_n(x)$ is the amplitude of the $n$th cosine component. $W(x)$ is the filter band weighting function, $T$ is the noise estimation. $\varepsilon$ is a small positive constant to prevent denominator from being 0, which is set to 0.001. $E_n(x)$ is the local energy function, and $E_n(x) = A_n(x) \cdot \Delta\varphi_n(x)$. $\Delta\varphi_n(x)$ is phase shift function and it can be calculated by

$$\Delta\varphi_n(x) = \cos[\varphi_n(x) - \bar{\varphi}(x)] - |\sin[\varphi_n(x) - \bar{\varphi}(x)]| \quad (3)$$

Here $\varphi_n(x)$ is the local phase of the Fourier transform at point $x$, and $\bar{\varphi}(x)$ is the weighted average of the local phases of all Fourier components at point $x$.

(6) The logarithmic Gabor filter is constructed and the amplitude feature of the image is extracted. Image amplitude feature extraction and filtering are carried out at the same time. In the frequency domain, the amplitude features are filtered by the logarithmic Gabor filter, and the obtained results perform the inverted Fourier transform. The amplitude features in different directions are weighted summation. Here, the weight values are set equal, that is, the sum average value is calculated. The obtained results are convoluted with the phase features, and the results are taken as the final amplitude features, which makes the features clearer.

(7) Color compensation is applied to the amplitude feature map. After the amplitude feature is filtered in frequency domain and is convoluted with phase feature, there will be some color distortion. The color information obtained in step two is used to compensate the amplitude feature. The processing model is given by equation (4).

$$F_{Ai}^*(m, n) = C_i(m, n) \cdot F_{Ai}(m, n) \qquad (4)$$

$$C_i(m, n) = \eta \log \left[ \frac{I_i(m, n)}{\sum_{i=1}^{3} I_i(m, n)} \right] \qquad (5)$$

Here $F_{Ai}(m, n)$ and $F_{Ai}^*(m, n)$ are the amplitude features before and after compensation, respectively. $i$ is the number of color channels, $C_i(m, n)$ is the color compensation coefficient of the $i$ color channel, and $\eta$ is compensation constant. The compensation coefficient $C_i(m, n)$ is an important parameter, whose value has a great influence on the color of the processing result. Under other conditions unchanged, the larger the value of $C_i(m, n)$ is, the larger the image color distortion will be, and the image will be darker. When its value is smaller, the color distortion will be smaller, and the image will be brighter. For different scene images, the effect is also different. After a large number of experiments and comparative analysis, the suitable range is from ten to thirty, i.e. $C_i(m, n) \in [10, 30]$, which can get better results for different

images. In the URSHR algorithm, its value is set to 20, i.e. $C_i(m, n) = 20$.

(8) The phase amplitude feature map is obtained. According to equation (6), phase feature and amplitude feature are fused together.

$$F_{AP}(m, n) = \alpha \cdot F_A(m, n) + \beta \cdot F_P(m, n) \qquad (6)$$

Here $F_{AP}(m, n)$ represents the fused phase amplitude feature, $F_A(m, n)$ is the amplitude feature, $F_P(m, n)$ is the phase feature. $\alpha$ and $\beta$ are the weighting coefficients, and $\alpha + \beta = 1$. Generally, $\alpha = \beta = 0.5$, but after a lot of experiments, we found that the value of $\beta$ is a little larger, which can effectively enhance the edge details. However, its value cannot be too large, otherwise it will have an over enhanced effect. After equilibrium consideration, their values are set to 0.45 and 0.55, respectively.

(9) The multi-scale Retinex theory is used to remove haze from urban remote sensing image. For the theoretical knowledge and application of Retinex, here is a brief introduction. If you want to understand the detailed reasoning process, please refer to literatures [1], [2], [9], [23]–[29], [38]. Assume that the obtained image $I(m, n)$ can be regarded as the result of multiplying by the incident light and the reflection of the object, it can be represented by the equation (7).

$$I(m, n) = L(m, n) \cdot R(m, n) \qquad (7)$$

Here $I(m, n)$ is the image obtained by the optical sensor, which is degraded by the influence of haze, and $(m, n)$ is the spatial position of the pixel point. $L(m, n)$ denotes the incident ambient light, i.e. the interference information to be removed. $R(m, n)$ denotes the reflected light on the surface of the object, which is the image information to be retained.

The logarithm operation is performed on both sides of equation (7) and then adjusted appropriately, and it can be rewritten into equation (8).

$$r(m, n) = \log[R(m, n)] = \log[I(m, n)] - \log[L(m, n)] \quad (8)$$

Here $L(m, n)$ is calculated by equation (9).

$$L(m, n) = G(m, n) * I(m, n) \qquad (9)$$

In equation (9), $G(m, n)$ is a Gaussian function, which is defined as follows.

$$G(m, n) = \frac{1}{2\pi\sigma^2} \exp(-\frac{m^2 + n^2}{2\sigma^2}) \qquad (10)$$

The parameter $\sigma$ is not only standard deviation of Gaussian function, but also is its scale parameter in equation (10).

The different value of scale parameter $\sigma$ has a great influence on the processing effect, and it is very difficult to achieve the best state of detail retention and color fidelity at the same time by adjusting and selecting a single parameter value, which is the shortage of the SSR algorithm. To overcome the defects of SSR algorithm and to achieve the goal of removing haze, protecting details and colors, this can be done by setting $M$ different parameter values, which is the MSR algorithm. The thought of the MSR algorithm is to weighted summation

of the results of the SSR algorithm taking different single scale parameter values, and then take it as the final processing result. Its definition is given in equation (11).

$$
\begin{cases}
r_{ji}(m, n) = \log[I_i(m, n)] - \log[G_j(m, n) * I_i(m, n)] \\
r_i(m, n) = \sum_{j=1}^{M} w_j r_{ji}(m, n)
\end{cases}
\tag{11}
$$

Here $i$ is the number of color channels, $i \in \{1, 2, 3\}$, which is corresponding to R, G and B channel of a color image. $M$ is the number of scale parameter values. $j$ denotes the $j$th scale parameter $\sigma$ in $M$ parameter values. $r_{ji}(m, n)$ is the reflection component of the $i$th color channel at the $j$ scale. $r_i(m, n)$ is the reflection component of the $i$ color channel processed by the Retinex algorithm, and $w_j$ is the weight of the scale parameter value.

At present, the atmospheric scattering model widely used for processing haze images was proposed by McCartney in 1976 [55], and the mathematical expression was given in equation (12).

$$
I(m, n) = J(m, n) \cdot t(m, n) + A \cdot [1 - t(m, n)]
\tag{12}
$$

Here $I(m, n)$ is the image affected by haze, namely, the image is obtained in haze weather. $J(m, n)$ is the image which is not affected by haze, i.e. haze-free image, which is obtained in sunny weather without haze. $(m, n)$ is the spatial position of pixels in the image, and $A$ is the ambient atmospheric light value, generally a constant. $t(m, n)$ is the transmittance of light in the atmosphere. Move the second term on the right of equation (12) to the left and divide it by $t(m, n)$ on both sides of the equation, and then the following equation can be obtained.

$$
J(m, n) = \frac{I(m, n) - A}{t(m, n)} + A
\tag{13}
$$

There are two parameters in equation (13), the ambient atmospheric light value $A$ and the atmospheric transmission $t(m, n)$. The values of these two parameters have a great influence on image haze removal. Therefore, almost all of these algorithms using scattering model to remove haze work on these two parameters estimation, different estimates bring different effects.

It can be seen in equation (13) that the image haze removal algorithm based on the atmospheric scattering model, in fact, estimates the haze-free image by acquiring the image affected by the haze. In essence, it is the same as the Retinex theory to remove haze, which is to reduce or eliminate the influence of ambient atmospheric light.

(10) Local histogram equalization is carried out. The MSR algorithm is used to remove the haze of the image, although it can get better results, but the overall tone is a little dark after processing. If the image is then processed with histogram equalization, it can make up for this deficiency. The histogram equalization processing can adjust the distribution of gray of an image, and it makes the processed image tone brighter. Therefore, the combination of the Retinex algorithm

and histogram processing can achieve complementary advantages. Avoiding color distortion, the RGB model image is transformed into the HSI model image, and then I component of the HSI model is processed. After processing, the HSI model image is converted to the RGB image again.

(11) Wavelet multi-scale decomposition and fusion processing are carried out. The wavelet multi-scale analysis theory is used to fuse the phase amplitude feature image and the haze removal result image. The fused results of them are taken as the final image haze removal results. It not only realizes haze removal, but also maintains rich detail information and clear contrast.

The obtained feature maps are decomposed by wavelet multi-scale theory, and each corresponding decomposition coefficients are fused separately. The final result is obtained by inverse wavelet transform. The determination of fusion rules is the key technology of each decomposition scale coefficient fusion. The URSHR algorithm will adopt pixel level strategy to complete fusion processing. After the two images are decomposed, several sub-images with high and low frequency coefficients will be obtained. For the low-frequency sub-image, the method of coefficient weighted summation is adopted for fusion processing. For the sub-image of high-frequency coefficients, the rule of 'grasping big and giving up small' is adopted for fusion processing. Suppose $I_1(m, n)$ and $I_2(m, n)$ represent two feature images processed by different methods respectively, and $I_F(m, n)$ represents the fused image. The mathematical model of weighted summation fusion rules of low-frequency coefficient sub-images are given in equation (14).

$$
I_F(m, n) = w_1 \cdot I_1(m, n) + w_2 \cdot I_2(m, n)
\tag{14}
$$

Here $w_1$ and $w_2$ represent the fusion weight of $I_1(m, n)$ and $I_2(m, n)$, i.e. the weighting coefficient, and $w_1 + w_2 = 1$. If $w_1 = w_2 = 0.5$, it is average weighted, namely the mean processing. By using this rule, the redundant information in the source image can be removed very well. For the source image with little difference, good results can be achieved with this rule. In the URSHR algorithm, the feature maps processed by two different ways come from the same remote sensing image, so their differences are very small, and the effect of fusion in this way is better than that in other ways.

For the fusion of sub-images of high-frequency coefficients on each decomposition scale, the fuse rule is 'grasping big and giving up small', and the mathematical model is given in equation (15).

$$
I_F(m, n) =
\begin{cases}
I_1(m, n); & I_1(m, n) \geq I_2(m, n) \\
I_2(m, n); & I_1(m, n) < I_2(m, n)
\end{cases}
\tag{15}
$$

(12) Output the final processed result.

## IV. DISCUSSION AND ANALYSIS OF EXPERIMENTAL RESULTS
### A. SCALE PARAMETER SETTING
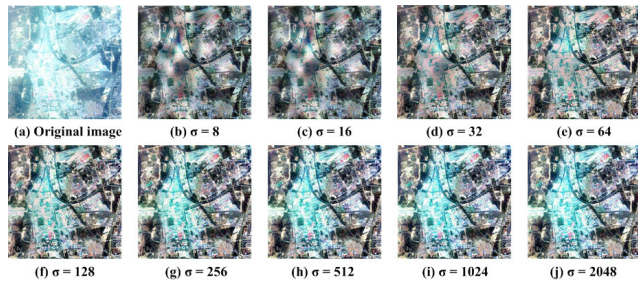In URSHR algorithm, the removal of haze mainly depends on MSR algorithm, which involves the determination of

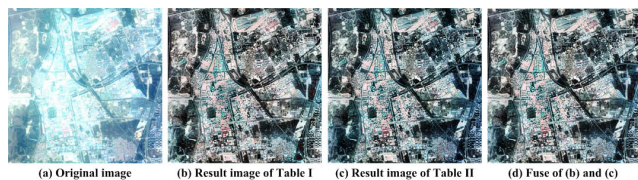**FIGURE 2.** Results obtained from single different scale parameter value of $\sigma$ in SSR method.



**FIGURE 3.** Results of different scale numbers in Table 1 and Table 2.

**TABLE 1.** Six scale parameters and their values.

| Scale parameter ( $\sigma$ ) | First scale | Second scale | Third scale | Fourth scale | Fifth scale | Sixth scale |
|---|---|---|---|---|---|---|
| Value | 20 | 40 | 60 | 80 | 100 | 120 |

**TABLE 2.** Nine scale parameters and their values.

| Scale parameter ( $\sigma$ ) | First scale | Second scale | Third scale | Fourth scale | Fifth scale |
|---|---|---|---|---|---|
| Value | 32 | 64 | 128 | 256 | 512 |
| Scale parameter ( $\sigma$ ) | Sixth scale | Seventh scale | Eighth scale | Ninth scale | |
| Value | 1024 | 2048 | 4096 | 8192 | |

the numbers and values of the scale parameter $\sigma$. Different number of parameters and different values will affect the filtering effect which is shown in Fig. 2 and Fig.3, and there was a detail discussion about the selection of the number of the parameter $\sigma$ for the SSR and MSR algorithms in [9]. Therefore, we directly adopted the scheme of scale parameter setting in [9], instead of discussing it in detail. The concrete parameter settings were shown in Table 1 and Table 2 and the corresponding experimental results were shown in Fig. 3. The image shown in Fig. 2(a) and Fig. 3(a) was the haze image, which was obtained by the QuickBird satellite. It can be seen from Fig. 2 that different single scale parameter values can obtain different processing results, which is shown in Figs. 2(b)-(j) in turn. Moreover, with the increase of parameter value, haze removal effect is better. But when the value reaches a certain value, changing a single value cannot continue to improve the ability of haze removal, which is the limitation of SSR algorithm.

The MSR algorithm breaks through the limitation of SSR algorithm by setting multiple scale parameter combinations. There are two ways to set the number of different parameter values, i.e. six or nine different values, as shown in Table 1 and Table 2. Only six scale parameters are set in Table 1, and the average sum of the processing results of them is shown in Fig. 3(b). Here their values are relatively small. This is because when the scale parameter value is smaller, it is beneficial to protect more details. However, at the same time, the haze removal effect is not good, the halo phenomenon and color distortion appear. To overcome this defect, nine scale parameters with larger values are set, as is shown in Table 2 and the experimental result is shown in Fig. 3(c). The scale parameter is large and the effect of haze removal is good, but the detail information will be lost. In the actual operation process, to achieve the purpose of removing haze and maintaining detailed information well, two parameter setting schemes are usually processed separately, and then the results are simply summed and averaged. This is the final results of the Retinex algorithm, which is shown in Fig. 3(d).

### B. EFFECT EVALUATION INDEX
The purpose of removing haze from remote sensing images is to reduce or eliminate the influence of haze on the detection of ground objects as much as possible, so the evaluation of haze removal effect is relative to the original haze image. The effect of haze removal is usually evaluated from two aspects: subjective evaluation and objective evaluation. The subjective evaluation depends on vision and experience, and it has strong individual factors. The objective evaluation is to judge the quality of processing results through some evaluation indicators, such as brightness, contrast, standard deviation, average value and information entropy. These indexes are some quantitative evaluation indexes, which are very scientific and can explain the problems well. This paper will use the structure similarity (SSIM), peak signal-to-noise ratio (PSNR) and contrast ratio (CR) to evaluate the haze removal effect from different levels. The structural similarity parameter reflects the restoration of image detail information, the peak signal-to-noise ratio reflects the haze removal ability, and the contrast ratio reflects the clarity of image. In practical application, subjective evaluation and objective evaluation are together used for comprehensive evaluation.

The structural similarity parameters are used to measure the similarity between two images, especially the information comparison of contour, edge and detail. Therefore, when the two images are very similar, their SSIM value is close to one. When the difference between them is large, the SSIM value is smaller. Because the image haze is eliminated, the more haze is removed, the better the result is. The greater the difference between the processed image and the original haze image is, the smaller the SSIM value is. The SSIM value is calculated by equation (16).

$$S = (l_{XY})^{\alpha} \cdot (c_{XY})^{\beta} \cdot (s_{XY})^{\gamma} \qquad (16)$$

Here $S$ represents the similarity degree between two images $X$ and $Y$. $X$ is the original image affected by haze, $Y$ is the filtered image, and their size is $M \times N$. $l_{XY}$, $c_{XY}$ and $s_{XY}$ represent the brightness, contrast and structure of the two images, respectively, in which the structure $s_{XY}$ is a leading factor. $\alpha$, $\beta$ and $\gamma$ represent the weight of each component, respectively. $l_{XY}$, $c_{XY}$ and $s_{XY}$ are calculated by the following equation.

$$\begin{cases} l_{XY} = \dfrac{2\mu_X\mu_Y + c_1}{\mu_X^2 + \mu_Y^2 + c_1} \\ c_{XY} = \dfrac{2\sigma_X\sigma_Y + c_2}{\sigma_X^2 + \sigma_Y^2 + c_2} \\ s_{XY} = \dfrac{\sigma_{XY} + c_3}{\sigma_X\sigma_Y + c_3} \end{cases} \quad (17)$$

In equation (17), $\mu_X$, $\mu_Y$, $\sigma_X$, $\sigma_Y$, $\sigma_X^2$ and $\sigma_Y^2$ represent the mean value, standard deviation and variance of the images $X$ and $Y$, respectively, and $\sigma_{XY}$ is the covariance between them. $X(m, n)$ and $Y(m, n)$ represent the gray value of a single pixel. $c_1$, $c_2$ and $c_3$ represent constants with very small values, respectively, avoiding the instability caused by zero denominator. The covariance coefficient $\sigma_{XY}$ can be got by equation (18).

$$\sigma_{XY} = \frac{1}{(M-1)\cdot(N-1)} \sum_{m=1}^{M} \sum_{n=1}^{N} [X(m,n) - \mu_X]$$
$$\cdot [Y(m,n) - \mu_Y] \quad (18)$$

If the weight coefficients satisfy $\alpha = \beta = \gamma = 1$, the constant is $c_3 = c_2/2$, and equation (16) can be rewritten as equation (19).

$$S = \frac{(2\mu_X\mu_Y + c_1)\cdot(2\sigma_{XY} + c_2)}{(\mu_X^2 + \mu_Y^2 + c_1)\cdot(\sigma_X^2 + \sigma_Y^2 + c_2)} \quad (19)$$

The PSNR reflects the error between the processed image and the original image, and the definition of its mathematical model is shown in equation (20).

$$P = 10 \cdot \log_{10}\left[\frac{(I_{fMAX})^2}{e_{MSE}}\right] \quad (20)$$

Here $e_{MSE}$ is the mean square error. Suppose that the original haze image is represented by $I_o$, the filtered image is represented by $I_f$, and their sizes are $M \times N$. The maximum gray value of the image $I_f$ is represented by $I_{fMAX}$. It can be seen in equation (20) that the larger the error between the filtered image and the original image, namely the larger the value $e_{MSE}$ is, the smaller the value $P$ of the PSNR is, indicating the better the haze removal effect. On the contrary, if the value of $e_{MSE}$ is smaller, the processed image is closer to the original image. Especially when it is the same as the original image, $e_{MSE} = 0$, the value of PSNR is infinite, and the ability to remove haze is the worst. $e_{MSE}$ is calculated by equation (21).

$$e_{MSE} = \frac{1}{M \cdot N} \sum_{m=1}^{M} \sum_{n=1}^{N} \left[I_f(m,n) - I_o(m,n)\right]^2 \quad (21)$$

The contrast ratio (CR) parameter of an image is used to describe the clarity of image details. The higher the CR value is, the clearer the image is. Its physical meaning is the ratio of black and white, namely, the gradient level from black to white. The higher the value, the clearer the gradient level is. Its mathematical calculation model is given by

$$C = \sum_{\delta} [\delta(i,j)]^2 P_\delta(i,j) \quad (22)$$

Here $i$ and $j$ represent the gray values of adjacent pixels, respectively. $\delta(i,j) = |i - j|$ is the gray difference between adjacent pixels, and $P_\delta(i,j)$ is the probability of occurrence of gray difference $|\delta(i,j)|$ of adjacent pixels.

## C. EXPERIMENTS OF URBAN REMOTE SENSING COLOR IMAGES

To verify the feasibility of the URSHR algorithm proposed in this paper, a series of experiments were carried out with real urban remote sensing haze images, and they were compared with different methods. Experimental data and results were shown in Fig. 4. The algorithms selected for comparative experiments include the histogram equalization (HE) method, the dark channel prior (DCP) method [3], the brightness preserving dynamic fuzzy histogram equalization (BPDFHE) method [8], the multi-scale model and histogram characteristic (MSMHC) method [9] and the new proposed URSHR algorithm in this paper. The selected experimental data were urban remote sensing images, and all of them were affected by haze to varying degrees, which was shown in Fig. 4. These original urban remote sensing haze images were shown in Figs. 4(A)-(J). The images shown in Fig. 4(A) and Fig. 4(B) were obtained by UAV. Their resolution is 2m and the image size is 795 × 553 and 490 × 330, respectively. Fig. 4(C) came from the QuickBird satellite. Its resolution is 2.5m and its size is 612 × 612. Figs. 4(D)-(J) were from the WorldView-3 satellite, but these images were processed and their resolution was 5m. The size of Fig. 4(D) and Fig. 4(E) is 600 × 600, and other image size is all 700 × 700. Figs. 4(a)-(e) show the experimental results obtained by different algorithms, respectively. And the corresponding methods are DCP, BPDFHE, HE, MSMHC and URSHR.

It can be seen in Fig. 4 that the DCP algorithm is not very effective in processing all urban remote sensing images and it cannot completely remove the haze of images, as shown in Fig. 4(a). The reason is that the DCP algorithm was proposed for outdoor images, and it was based on atmospheric scattering model, in which the atmospheric transmittance $t(m, n)$ was calculated by depth of field. For remote sensing images, the depth of field span is relatively small and it can be ignored. However, for outdoor images, the depth of field span is generally large and the impact is uneven, so it is necessary to have a more accurate estimation to get good results. When using the DCP algorithm to remove the haze of remote sensing image, the same parameters are set uniformly, which may be the bad experimental results caused by inaccurate parameter estimation. At the same time, the urban remote
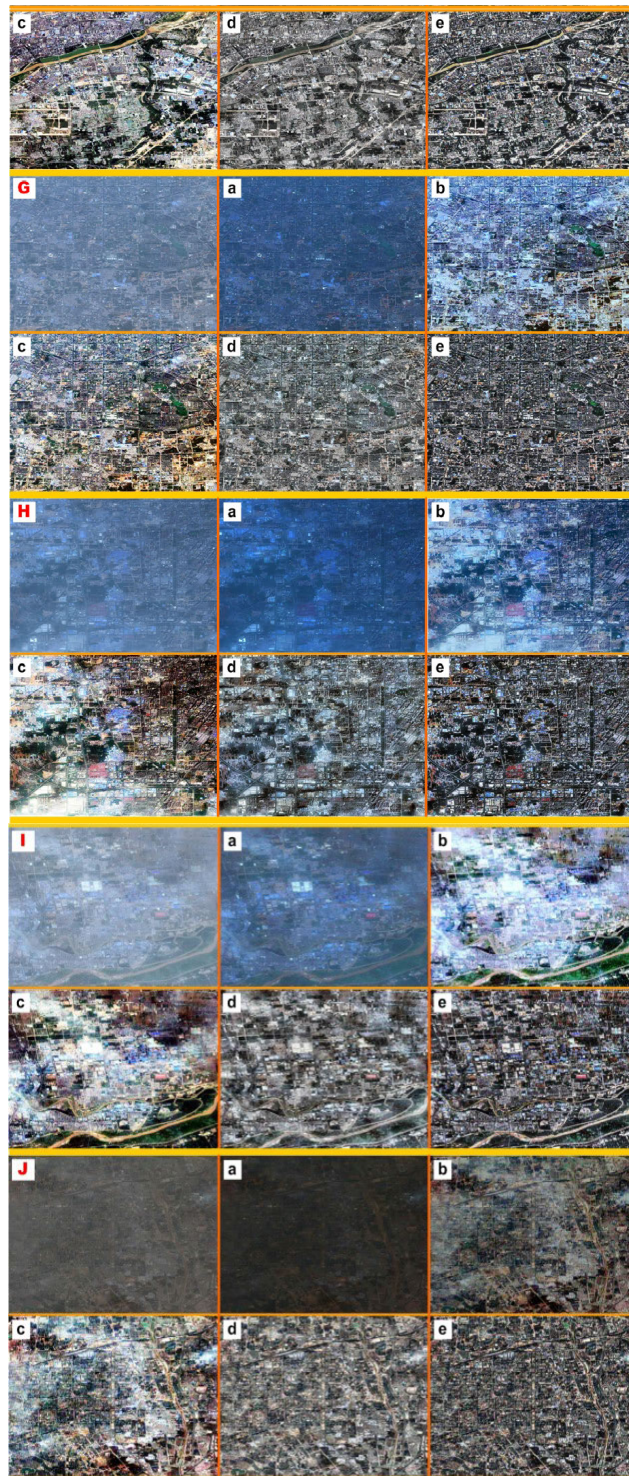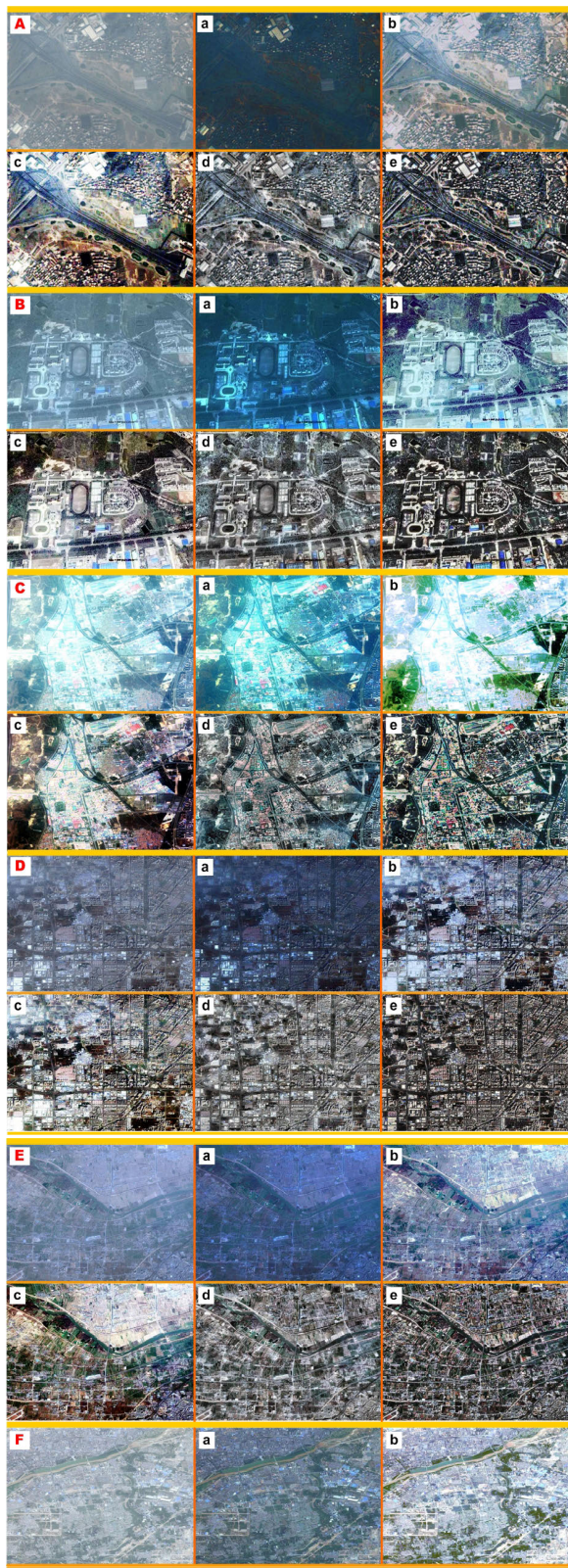
**FIGURE 4.** Experimental results obtained by different algorithms. A-J represents the original urban remote sensing haze image, and a-e represents the experimental results obtained by DCP, BPDFHE, HE, MSMHC and URSHR method, respectively.



**FIGURE 4.** *(Continued.)* Experimental results obtained by different algorithms. A-J represents the original urban remote sensing haze image, and a-e represents the experimental results obtained by DCP, BPDFHE, HE, MSMHC and URSHR method, respectively.

sensing images mainly contain artificial buildings, including a large number of white or gray walls and roofs. This does not meet the assumptions of the DCP algorithm, and also affects

the performance and effect of the DCP algorithm. In addition, the color of urban remote sensing image processed by the DCP algorithm is a little dark.

Throughout all the experimental results, the BPDFHE algorithm can maintain good brightness, which is shown in Fig. 4(b). From the visual point of view, although the BPDFHE algorithm can get higher brightness and better hue, the haze removal in the image is obviously poor. This shows that the algorithm can be used to enhance the image tone, especially the shadow and backlight processing. However, it is not its advantage to remove the haze of an image; namely, the haze removal ability is relatively weak.

The HE algorithm is a very effective image enhancement method, which is often used to measure the quality of other algorithms. It can be seen in Fig. 4(c) that after the urban remote sensing image is processed by the HE algorithm, the hue will become bright, which is very similar with the BPDFHE algorithm. In terms of haze removal, sometimes the effect is very good, e.g., the processing of Figs. 4(A)-(G). However, sometimes the haze removal effect is not ideal, for example, for the processing results of Figs. 4(H)-(J). The HE algorithm can enhance the image by adjusting the gray dynamic range of the image, so if the remote sensing image contains a relatively uniform haze, it can effectively remove haze. If the haze contained in the image is thick or distributed unevenly, it is very difficult for the HE algorithm to eliminate the haze. In addition, it can be seen in Fig. 4(c) that the color of the image processed by the HE algorithm is a little distorted and over enhanced.

The MSMHC algorithm is a good algorithm for remote sensing image haze removal, and the processing results are shown in Fig. 4(d). In addition, for the remote sensing images of other land natural scenes, it can also obtain better haze removal results, which was discussed in [9]. But its disadvantage is that when it processes urban remote sensing images, because there is more abrupt edge information, it is easy to produce halo phenomenon, which can be seen clearly in Fig. 4(d).

For the urban remote sensing haze images, in addition to effectively removing the haze, it is also necessary to retain as much detail and edge information as possible, which is of great significance for the subsequent feature extraction and interpretation. It can be seen in Fig. 4(d) that although the MSMHC algorithm can effectively remove haze, the details are not rich enough and there is halo phenomenon. Therefore, on this basis, this paper proposed the URSHR algorithm for urban remote sensing image haze removal. From the experimental results shown in Fig. 4(e), it is shown that the URSHR algorithm is indeed an effective method for urban remote sensing image haze removal, which can not only remove haze, but also obtain the enhanced edge and other details, and it can overcome the halo phenomenon in the image.

Judging from the visual effect, for the haze removal of urban remote sensing images, the URSHR algorithm is the best, the followed better methods are the MSMHC and HE algorithms. With the different haze thickness, the HE
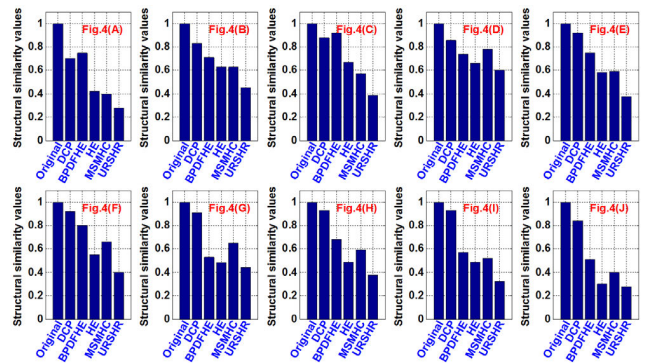


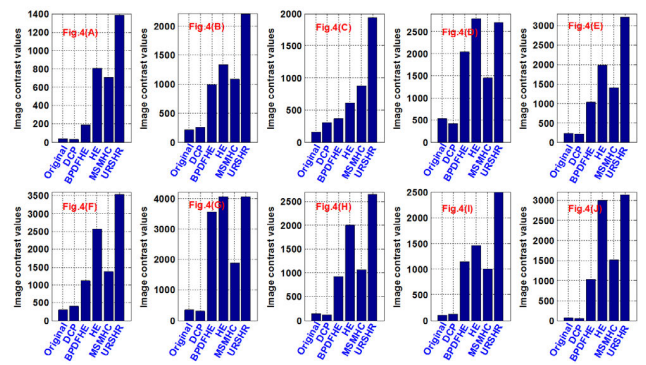**FIGURE 5.** SSIM values of different images and methods.



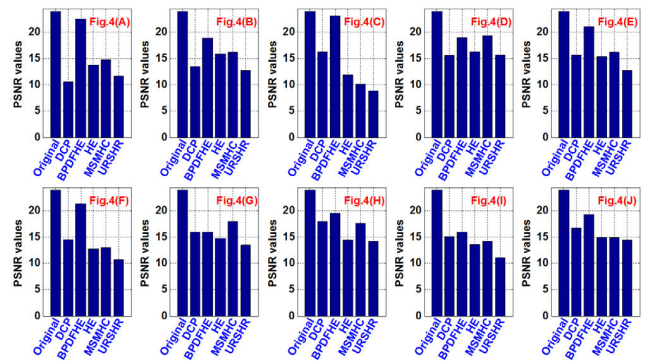**FIGURE 6.** CR values of different images and methods.



**FIGURE 7.** PSNR values of different images and methods.

algorithm has different removal effect. Finally, it is the BPDFHE and DCP algorithms. Next, the performance of the above five methods is evaluated from the perspective of quantitative analysis. There are three quantitative evaluation parameters for analysis, namely SSIM, CR and PSNR. For each image shown in Fig. 4, their parameter values were calculated respectively and the comparative analysis was carried out. The results were shown in from Fig. 5 to Fig. 7.

The experimental results of the SSIM parameter were shown in Fig. 5. It can be seen in Fig. 5 that the SSIM parameter value of the original image is one and the value obtained by the URSHR algorithm is the minimum. This means that the image processed by the URSHR algorithm is

quite different from the original haze image, but it is closer to the image which is not affected by haze. This shows that the URSHR algorithm has a strong ability to remove haze and can achieve good results. Then, the smaller SSIM values are the HE and MSMHC algorithms, which shows that the two algorithms have general ability to remove haze. The SSIM values obtained by the DCP algorithm is very close to that of the original haze image, which shows that the DCP algorithm is not suitable for dealing with the haze problem in the urban remote sensing image. The SSIM values of the BPDFHE method is in the middle, and it indicates that it is in the middle of the haze removal level.

The contrast ratio (CR) of an image can fully reflect the level sense of image detail, namely, the clarity degree of image detail information. It can be seen in Fig. 6 that in addition to the DCP algorithm, other algorithms can obtain high CR values, especially the HE and URSHR algorithms. In general, the MSMHC algorithm can obtain relatively stable image CR values, but the values are not particularly high, so the details are not much clear. For all urban remote sensing images processing, the URSHR algorithm can get the highest CR values and the best definition. The CR values of images processed by the URSHR algorithm are usually dozens of times of the original image and several times of other algorithms. It shows that the image processed by the URSHR algorithm is quite different from the original haze image, not only the haze is effectively removed, but also the more clear details are obtained. Therefore, the URSHR algorithm is an effective haze removal algorithm, and it is also suitable for urban remote sensing image processing. Therefore, the URSHR algorithm is very excellent in terms of clarity and gradient level sense.

In addition, there is an abnormal phenomenon in Fig. 6 that the CR value of HE method in Fig.4 (D) and Fig.4 (G) is a little higher than that of URSHR method. There are two reasons. On the one hand, the HE method improves the contrast by adjusting and stretching the gray value range of these two images. On the other hand, the haze distribution of these two images is uniform and relatively thin, which is exactly the best condition for HE algorithm to remove haze, so it can obtain the best effect and good contrast.

Because the PSNR value is compared with the original haze image, the PSNR value of all the original images is infinite. To facilitate comparative analysis, the PNSR value of the original image is set to the maximum constant, and here the value is set to 24, as shown in Fig. 7. It has been analyzed that the larger the PSNR value is, the worse the haze removal ability is. It is known in Fig. 7 that the PNSR values of images obtained by the BPDFHE algorithm is almost the largest, which shows that although it can maintain the brightness of the image well, the haze removal ability is weak. Next, the PNSR values of the DCP algorithm is larger, followed by the MSMHC and HE algorithms, and the least PNSR value is the URSHR algorithm. This further proves that the URSHR algorithm has the best ability to remove haze. From the point of view of noise removal, the URSHR algorithm is a very

effective and good method for urban remote sensing image haze removal and preprocessing.

In above three evaluation parameters, the urban remote sensing haze image processed by the URSHR algorithm not only has the lowest PNSR and SSIM values, but also has all almost the highest CR values, which fully shows that the algorithm can effectively remove haze and get rich details and good clarity.

## D. EXPERIMENTS OF PANCHROMATIC AND MULTISPECTRAL URBAN REMOTE SENSING IMAGES

In the above part, these comparative experiments were carried out for the color urban remote sensing images. Next experiments are carried out for panchromatic, single band multispectral and color multispectral images, which are important remote sensing image data. To satisfy the needs of scientific research, remote sensing satellites can usually obtain multispectral and panchromatic images at the same time. But their spatial resolution is different. The spatial resolution of panchromatic images is higher than that of multispectral images. Two sets of images from the GeoEye-1 satellite and the WorldView-3 satellite are used in the next experiments. Both of them are high-resolution satellites and include one panchromatic remote sensing image and four bands multispectral remote sensing images. The experimental images are shown in Fig. 8. The size of the original image is too large, so their size is cut to $1000 \times 1000$. These images shown in Fig. 8(a) came from the GeoEye-1 satellite. Fig. 8(A) is the second band multispectral image with a spatial resolution of 2m, and Fig. 8(B) is a panchromatic image of the same region with a spatial resolution of 0.5 m. Fig. 8(C) is synthesized by bands 1, 2 and 3, Fig. 8(D) is synthesized by bands 3, 2 and 1, and Fig. 8(E) is synthesized by bands 3, 2 and 4, respectively. The order of the bands in turn represents the R, G, and B channel images. The image shown in Fig. 8(F) is a false color image synthesized by all four band multispectral images. The spatial resolution of four color images (Figs. 8(C)-(F)) is 2m. The images shown in Fig. 8(b) came from the WorldVied-3. The spatial resolution of the panchromatic image (Fig. 8(G)) is 0.31m, and the resolution of other multispectral images (Figs. 8(H)-(K)) is 1.24m. Fig. 8(H) is the first band image, Fig. 8 (I) is composed of 1, 2, 3 bands, and Fig. 8(J) is composed of 4, 2, 1 bands. Fig. 8(K) is a false color image composed by all bands 1-4. There are more haze and uneven in the images shown in Fig. 8(a). But in Fig. 8(b), the haze contained in these images is relatively uniform and very thin. The two groups of data were processed and compared by the DCP, BPDFHE, HE, MSMHC and URSHR methods, respectively. And their experimental results were shown in Fig. 9.

It is very clear in Fig. 9 that the BPDFHE algorithm is not suitable for processing panchromatic and single band images. Because these images are processed by the BPDFHE algorithm, not only their clarity is obviously reduced, but also their hue also becomes very dark. For color multispectral images, the BPDFHE algorithm can maintain and enhance the
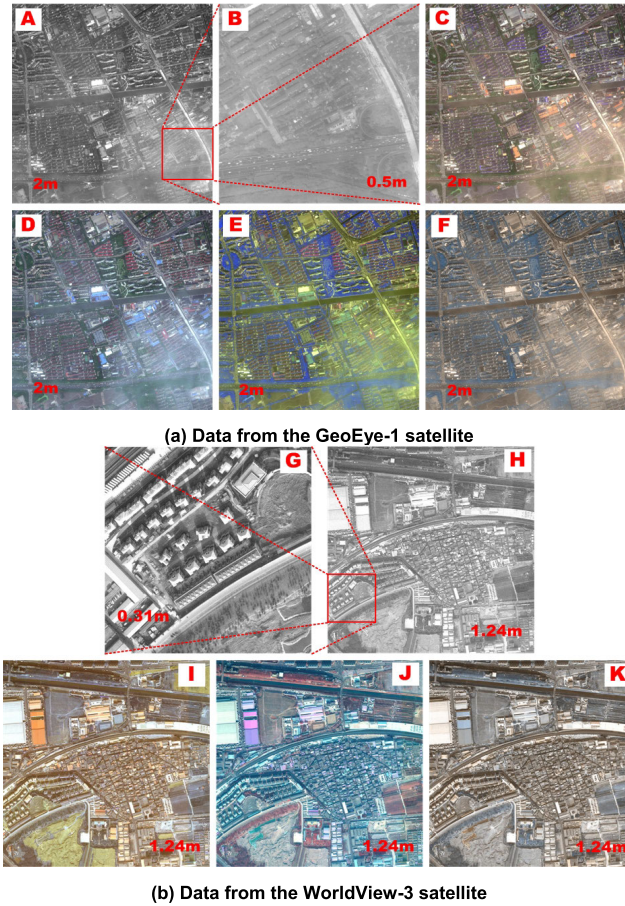
(a) Data from the GeoEye-1 satellite



(b) Data from the WorldView-3 satellite

**FIGURE 8.** Experimental data of panchromatic and multispectral images. B and G are panchromatic gray images with resolutions of 0.5m and 0.31m respectively, A and H are single band gray images with resolutions of 2m and 1.24m respectively, C. D, E and F are color images synthesized from multispectral images with a spatial resolution of 2m, I, J and K are multispectral color images with a spatial resolution of 1.24m.

brightness of the image, but it also maintains the brightness of haze, so it has a weak ability to remove the haze in multispectral images, which is shown in Fig. 9(b). When there are more hazes in panchromatic and gray images, the DCP algorithm is also not suitable to deal with them, because this kind of image does not meet the precondition of DCP algorithm. For multispectral color images, the DCP algorithm can remove some haze, but the removal effect and ability are very limited, as is seen in Fig. 9(a). Using the HE method to deal with haze image, when the haze in the image is more uniform, it can get a better effect, as shown in Figs. 9(G)(c)-(K)(c). When the haze in the image is uneven, the processing effect is not ideal, which is shown in Figs. 9(A)(c)-(F)(c). The HE algorithm is to achieve image enhancement and haze removal by stretching the gray range of the image. In the area where haze exists, the image is relatively bright, so when the HE algorithm is used, this part will become brighter, and the dark area will be darker, resulting in poor final effect. For MSMHC algorithm, whether it is panchromatic images, gray
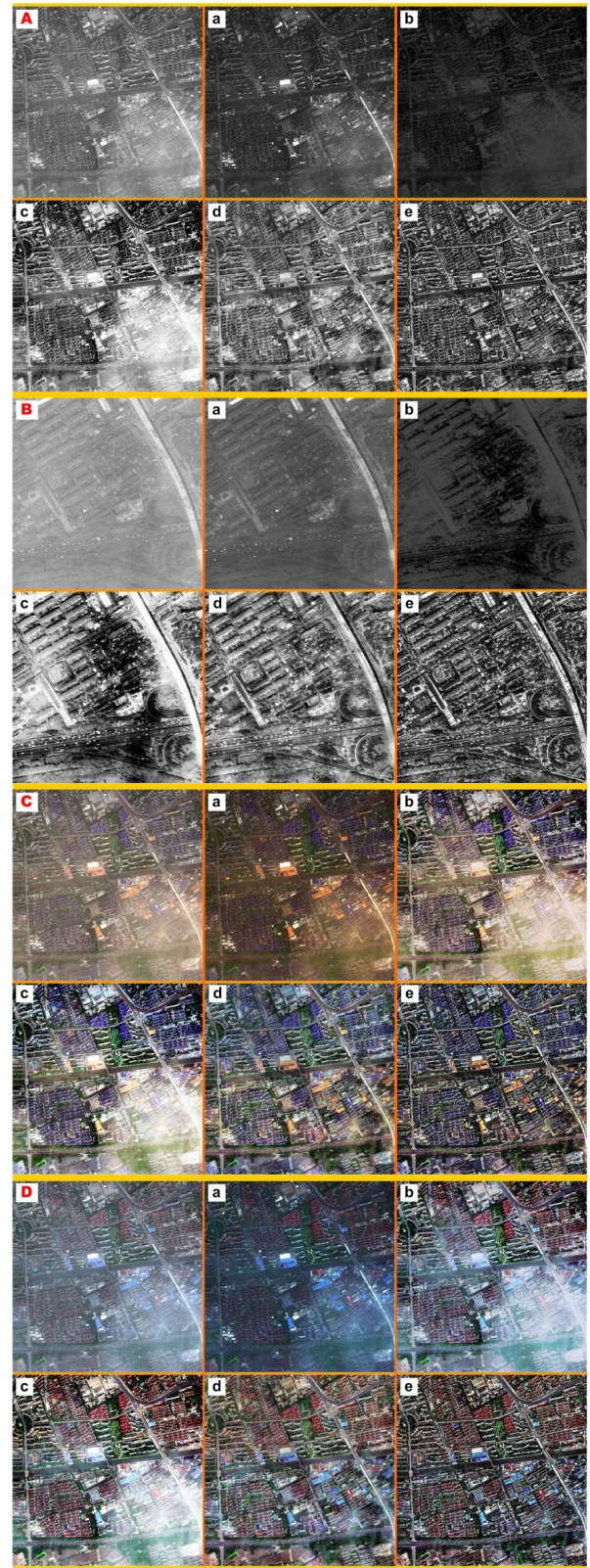


**FIGURE 9.** Experimental results of panchromatic and multispectral images. A-K are original remote sensing image, B, G are panchromatic images, A, H are single multispectral images, C, D, E, F, H, I, J and K are color multispectral images, and a-e represents the experimental results obtained by DCP, BPDFHE, HE, MSMHC and URSHR method, respectively.
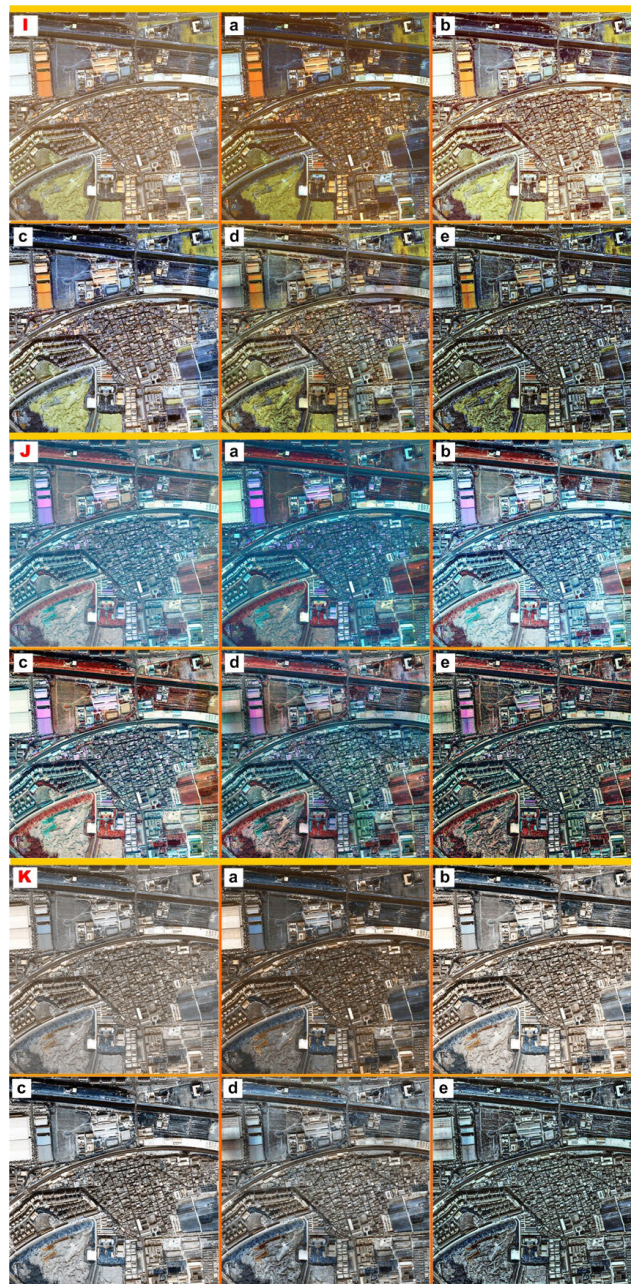
**FIGURE 9.** *(Continued.)* Experimental results of panchromatic and multispectral images. A-K are original remote sensing image, B, G are panchromatic images, A, H are single multispectral images, C, D, E, F, H, I, J and K are color multispectral images, and a-e represents the experimental results obtained by DCP, BPDFHE, HE, MSMHC and URSHR method, respectively.
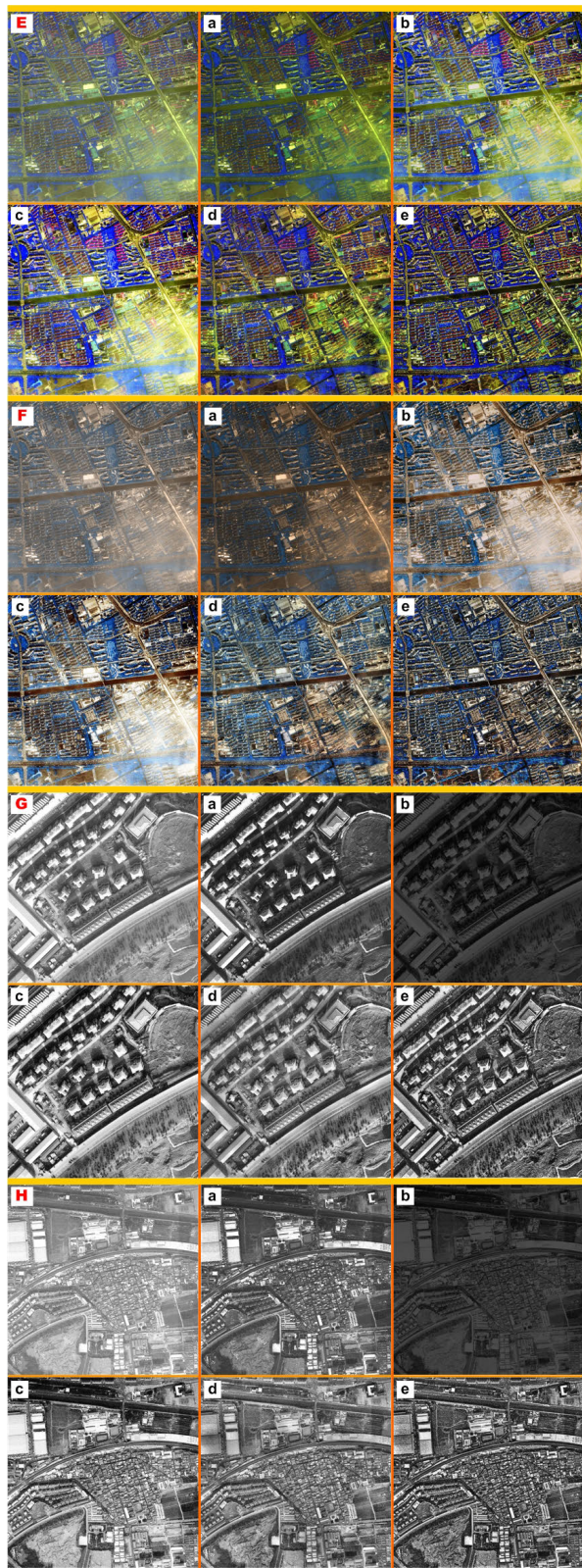
**FIGURE 9.** *(Continued.)* Experimental results of panchromatic and multispectral images. A-K are original remote sensing image, B, G are panchromatic images, A, H are single multispectral images, C, D, E, F, H, I, J and K are color multispectral images, and a-e represents the experimental results obtained by DCP, BPDFHE, HE, MSMHC and URSHR method, respectively.

and color multispectral images, whether it is uniform haze or non-uniform haze images, it can remove the haze phenomenon in the image well, as shown in Fig. 9(d). At the same time, we can also see it in Figs. 9(A)(d)-(F)(d), when the values of the two sides of the edge information are quite different, halo phenomenon is easy to appear. As shown in Fig. 9(e), it is very clear that the URSHR algorithm can

not only effectively remove haze in panchromatic and single band multispectral remote sensing images, but also obtain very good detail information and contrast. At the same time, the URSHR algorithm can obtain good experimental results for the color multispectral images synthesized by different bands with any order, as well as the false color images synthesized by all single band images. It shows that the number of bands and the order of the bands do not affect the effectiveness of the URSHR algorithm.

After the above visual analysis and judgment, it is concluded that the URSHR algorithm is very good and suitable for dealing with haze in panchromatic or multispectral urban remote sensing image. Next, we also use the quantitative evaluation factors PSNR, SSIM and CR to compare and analyze the experimental results which are shown in Fig. 9, and the evaluation parameter values of these images are shown in Fig. 10, Fig. 11 and Fig. 12, respectively. The precision result values of some of these parameters are shown in Table 3.
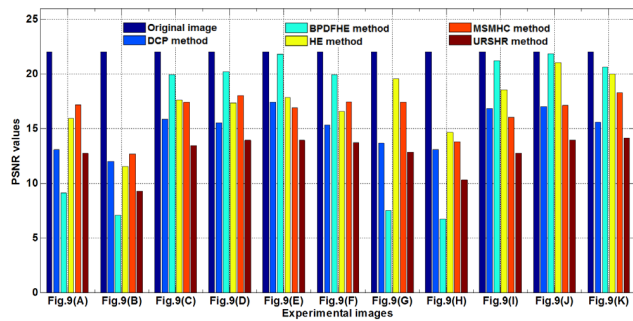


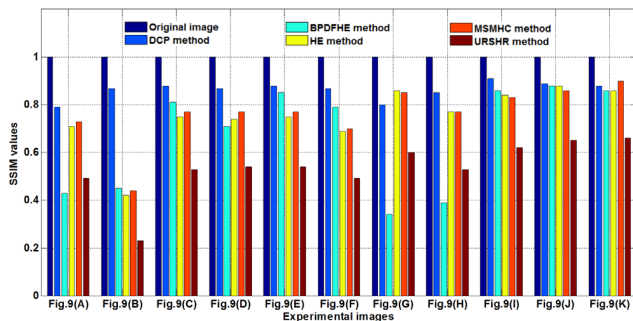**FIGURE 10.** PSNR comparison of panchromatic and multispectral images.



**FIGURE 11.** SSIM comparison of panchromatic and multispectral images.

Because the PSNR value of the original haze image is infinite, for the convenience of comparative analysis, in Fig. 10, the value is set to 22, which is greater than that of other images, i.e. the maximum value. For color multispectral images, the PSNR value of the BPDFHE algorithm is large, which indicates that the ability to remove haze is relatively weak. As we have analyzed before, the BPDFHE algorithm is not suitable for processing panchromatic and single band gray images, so the image quality after processing with it is very poor, resulting in a very low PSNR value.
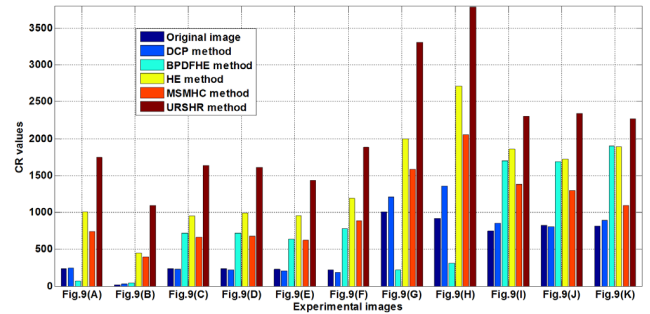


**FIGURE 12.** CR comparison of panchromatic and multispectral images.

**TABLE 3.** Comparison of different parameters results of some processed panchromatic and multispectral images.

| Image | Method | PSNR | SSIM | CR |
|---|---|---|---|---|
| Fig.9(G)(a) | DCP | 13.65 | 0.80 | 1209 |
| Fig.9(G)(b) | BPDFHE | 7.52 | 0.34 | 223 |
| Fig.9(G)(c) | HE | 19.56 | 0.86 | 1995 |
| Fig.9(G)(d) | MSMHC | 17.38 | 0.85 | 1589 |
| Fig.9(G)(e) | URSHR | 12.85 | 0.60 | 3304 |
| Fig.9(H)(a) | DCP | 13.04 | 0.85 | 1357 |
| Fig.9(H)(b) | BPDFHE | 6.72 | 0.39 | 306 |
| Fig.9(H)(c) | HE | 14.65 | 0.77 | 2714 |
| Fig.9(H)(d) | MSMHC | 13.76 | 0.77 | 2050 |
| Fig.9(H)(e) | URSHR | 10.32 | 0.53 | 3788 |
| Fig.9(I)(a) | DCP | 16.87 | 0.91 | 858 |
| Fig.9(I)(b) | BPDFHE | 21.17 | 0.86 | 1699 |
| Fig.9(I)(c) | HE | 18.53 | 0.84 | 1861 |
| Fig.9(I)(d) | MSMHC | 16.00 | 0.83 | 1379 |
| Fig.9(I)(e) | URSHR | 12.73 | 0.62 | 2304 |
| Fig.9(J)(a) | DCP | 17.02 | 0.89 | 808 |
| Fig.9(J)(b) | BPDFHE | 21.87 | 0.88 | 1692 |
| Fig.9(J)(c) | HE | 21.00 | 0.88 | 1724 |
| Fig.9(J)(d) | MSMHC | 17.12 | 0.86 | 1294 |
| Fig.9(J)(e) | URSHR | 13.91 | 0.65 | 2343 |
| Fig.9(K)(a) | DCP | 15.56 | 0.88 | 892 |
| Fig.9(K)(b) | BPDFHE | 20.63 | 0.86 | 1901 |
| Fig.9(K)(c) | HE | 19.96 | 0.86 | 1895 |
| Fig.9(K)(d) | MSMHC | 18.28 | 0.90 | 1098 |
| Fig.9(K)(e) | URSHR | 14.18 | 0.66 | 2271 |

In other normal cases, the lowest PSNR value is the URSHR algorithm for all multispectral urban remote sensing images, as shown in Fig. 10. It shows that the haze removal ability of the URSHR method is relatively strong, and it can remove haze very well. The next method is the MSMHC and DCP algorithm.

Among the SSIM values shown in Fig. 11, the URSHR algorithm has the smallest value, indicating that it has the largest gap with the original image, and its haze removal effect is the most obvious and clean. The largest SSIM value is DCP algorithm, which shows that its overall structure is the closest to the original image, and its effect on haze removal of

urban panchromatic and multispectral remote sensing image is not ideal. The SSIM values of MSMHC, BPDFHE and HE algorithms are close, which shows that the removal effect of haze is similar.

The CR values of panchromatic and multispectral images are shown in Fig.12. In either case, the value of the URSHR algorithm is the largest, which shows that it can effectively keep the details of the image and improve the clarity of the image. And the spatial resolution of these two experimental images is very high. It shows that the URSHR algorithm can be used to deal with haze in high-resolution urban remote sensing image. Next, the image obtained by the HE algorithm has high CR value, but compared with the URSHR algorithm, there is a big range. This shows that the ability of HE algorithm to improve the image clarity is limited.

The Fig. 9(G) is a panchromatic image and tis resolution is 0.31m, and the resolution of other images from Fig. 9(H) to Fig. 9(K) is 1.24m. The Fig. 9(H) is single band gray image, and other images of Figs. 9(I)-(K) are RGB color images synthesized by single multispectral image. All of them came from the WorldView-3 satellite. Because of the typical representativeness of these five images, their evaluation parameter values are given in Table 3. It can be seen in Table 3 that except for the abnormal processing of panchromatic and grayscale images by BPDFHE algorithm, in other cases, SSIM values and PSNR values of the URSHR algorithm are the minimum, and its CR value is the maximum. For example, in Fig. 9(J), the SSIM, PSNR and CR value is 0.65, 13.91 and 2343, respectively.

The ability of image detail preserving is generally described by edge saved index (ESI). The higher the ESI value is, the better the edge is saved. The edge saved index is divided into horizontal ESI and vertical ESI, and their definition models are shown in equation (23) and equation (24), respectively.

$$HESI = \frac{\sum_{m=1}^{M} \sum_{n=2}^{N-1} |I_{F-L}(m, n-1) - I_{F-R}(m, n+1)|}{\sum_{m=1}^{M} \sum_{n=2}^{N-1} |I_{O-L}(m, n-1) - I_{O-R}(m, n+1)|} \quad (23)$$

$$VESI = \frac{\sum_{m=2}^{M-1} \sum_{n=1}^{N} |I_{F-U}(m-1, n) - I_{F-D}(m+1, n)|}{\sum_{m=2}^{M-1} \sum_{n=1}^{N} |I_{O-U}(m-1, n) - I_{O-D}(m+1, n)|} \quad (24)$$

Here *HESI* and *VESI* represent the horizontal ESI and the vertical ESI, respectively. The size of an image is represented by $M \times N$. $I_{F-L}, I_{F-R}, I_{F-U}, I_{F-D}$ respectively represent the gray value of the neighboring pixels of left and right or upper and down at the edge junction of the image after removing the haze. $I_{O-L}, I_{O-R}, I_{O-U}, I_{O-D}$ are gray values of adjacent pixels at the edge pixel of the original remote sensing image. From equations (23) and (24), ESI is the ratio of the haze removed image to the original image. Therefore, the ESI value of the original image itself is equal to one. Compared
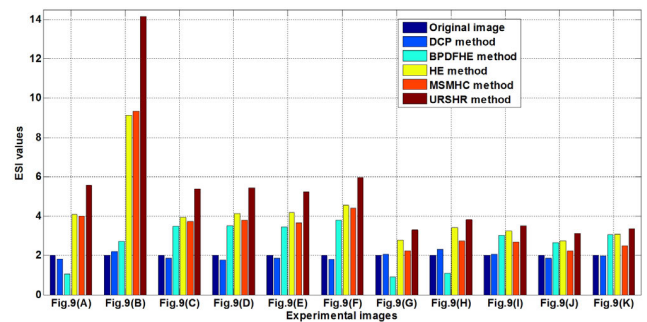


**FIGURE 13.** ESI comparison of panchromatic and multispectral images.

with the original haze image, if the haze removal image has more detailed information, its ESI value is larger. To facilitate the analysis, when calculating the edge saved index, the horizontal ESI and the vertical ESI are combined, namely, *ESI = HESI + VESI*. The ESI values of all experimental images (Figs. 9(A)-(K)) are shown in Fig. 13.

It can be seen in Fig. 13 that for Fig. 9(B) image, the HE, MSMHC and URSHR algorithms obtain high ESI values. Through Fig. 9(B), it is known that the image contains a lot of haze, and just these three methods can effectively remove the haze and obtain more detailed information. Therefore, their ESI values are high, especially the URSHR algorithm. In other images, the ESI value of URSHR algorithm is still the highest. This fully shows that after the urban remote sensing haze image is processed by URSHR algorithm, the haze is indeed removed, and a large number of geometric details are retained in the processed image. For color image, the BPDFHE, HE and MSMHC algorithms can get close ESI values, but for gray images or panchromatic images, the ESI value of BPDFHE algorithm is relatively low. This shows that the BPDFHE algorithm is not very stable. In addition, the ESI value of the DCP algorithm is very close to that of the original image.

Through the above detailed analysis, it can be concluded that the URSHR algorithm can effectively remove the haze in high-resolution panchromatic and multispectral urban remote sensing images, not only the haze removal effect is good, but also the rich detail information is retained, and the contrast has been significantly improved. Moreover, the URSHR algorithm has the better robustness.

### E. EXPERIMENTS OF OBTAINING PHASE CONSISTENCY FEATURE IMAGES

As mentioned earlier, the MSMHC algorithm is a good remote sensing image haze removal algorithm. But the algorithm also has its imperfections. For example, for urban remote sensing image, if there are some details or edge mutation, the algorithm is easy to produce image halo phenomenon. In the aspect of haze removal, the MSMHC algorithm is better than the HE algorithm, but sometimes it is not better than the HE algorithm in detail keeping. To improve the shortcomings of the MSMHC algorithm, according to
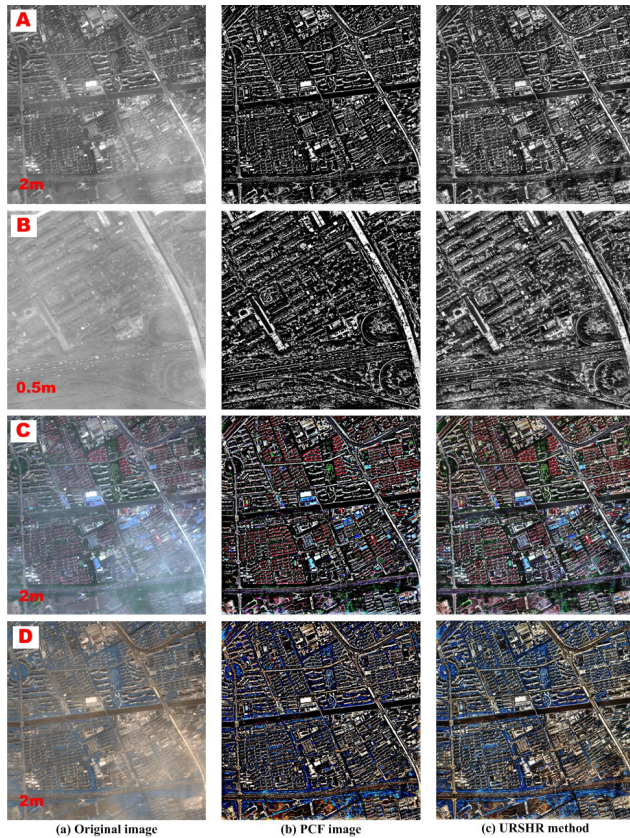
**FIGURE 14.** PCF feature extraction results.

(a) Original image     (b) PCF image     (c) URSHR method



**FIGURE 15.** Experimental results of outdoor haze images. A, B is the original outdoor haze image, and a-e represents the experimental results obtained by DCP, BPDFHE, HE, MSMHC and URSHR method, respectively.

the characteristics of urban remote sensing image, this paper proposed to use the phase consistency feature of the image to remove the haze of urban remote sensing image. The phase consistency feature is the reflection of the spatial distribution of the feature of the object, which is not affected by the haze. Obtaining the phase consistency feature of image is not only an important part of the URSHR algorithm, but also a key step of it. Therefore, the following experiment is to discuss the phase consistency feature (PCF) acquisition of urban remote sensing image. And the experimental results were shown in Fig. 14. Here Fig. 14(a) is the original remote sensing image, Fig. 14(b) is the PCF image and Fig. 14(c) is the result image obtained by the URSHR method. The PCF feature map is obtained by convolution of phase and amplitude features and fusion processing, and color supplementary processing is carried out for color image. The feature of PCF is that the contour information is very clear, which is similar to the edge sharpening enhancement processing. Because the phase consistency information is extracted, the edge and contour information is mainly extracted, and other information is discarded seriously. But the URSHR algorithm uses this advantage to enhance the detail information of haze image.

### F. EXPERIMENTS OF OUTDOOR HAZE IMAGES

The URSHR algorithm is specially proposed for urban remote sensing images, because it uses the phase consistency
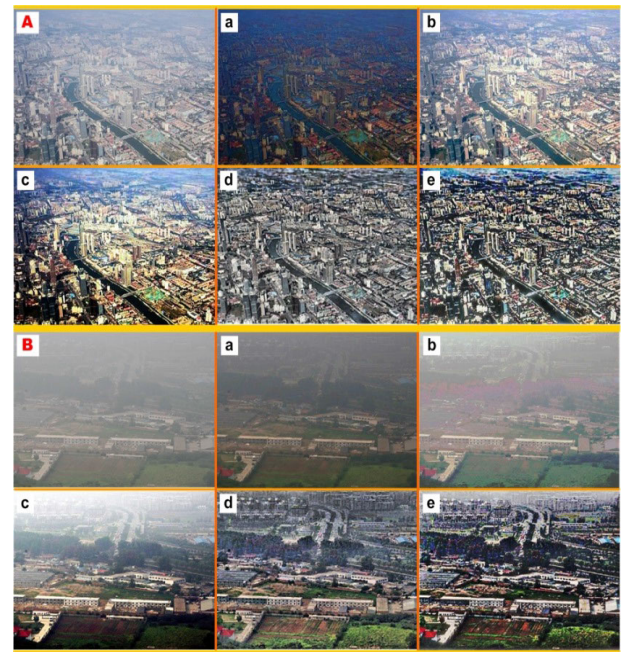
of an image, which can provide good structural features and contour information, so it has better advantages in processing urban remote sensing image. Let's discuss the situation that is not urban remote sensing image, including two cases: (1) outdoor images, (2) remote sensing images of natural or countryside scene.

Firstly, the haze removal of outdoor images was studied and analyzed. The experimental data and results were shown in Fig. 15. Two original outdoor haze images were shown in Fig. 15(A) and Fig. 15(B), and their size was $400 \times 280$ and $426 \times 373$, respectively. The results got by the DCP, BPDFHE, HE, MSMHC and URSHR algorithms were shown in from Fig. 15(a) to Fig. 15(e) in order. It can be seen in Fig. 15 that the URSHR algorithm can also process outdoor images with more artificial buildings, but the far scene part of the processing is not ideal, as shown in Fig. 15(e). The other four methods can also remove the haze in the outdoor images in different degrees. Table 4 is the relevant evaluation parameter values of the images shown in Fig. 15. It is known in Table 4 that the evaluation results of the obtained images reflect the same law as the analysis of urban remote sensing image in Section IV.C and IV.D. The PSNR values of the images processed by the BPDFHE method is the highest, and they are 22.79 (Fig. 15(A)(b)) and 27.14 (Fig. 15(B)(b)), respectively. It shows that the ability of removing haze of the BPDFHE method is poor. The lowest PSNR value is obtained by the DCP or URSHR algorithms, their results are shown in Fig. 15(A)(a) and Fig. 15(B)(e), respectively, and the corresponding values is is 8.85 and 9.77. The SSIM values are still the minimum of the URSHR algorithm, which shows that

**TABLE 4.** Comparison of different parameters of outdoor image processing results.

| Image | Method | PSNR | SSIM | CR |
|-------|--------|------|------|-----|
| Fig.15(A)(a) | DCP | 8.85 | 0.61 | 337 |
| Fig.15(A)(b) | BPDFHE | 22.79 | 0.86 | 1200 |
| Fig.15(A)(c) | HE | 13.54 | 0.59 | 2811 |
| Fig.15(A)(d) | MSMHC | 13.12 | 0.62 | 1863 |
| Fig.15(A)(e) | URSHR | 9.17 | 0.34 | 5969 |
| Fig.15(B)(a) | DCP | 14.30 | 0.84 | 55 |
| Fig.15(B)(b) | BPDFHE | 27.14 | 0.76 | 87 |
| Fig.15(B)(c) | HE | 13.13 | 0.53 | 539 |
| Fig.15(B)(d) | MSMHC | 13.00 | 0.34 | 810 |
| Fig.15(B)(e) | URSHR | 9.77 | 0.18 | 2568 |

there is the largest difference between the processed images by the URSHR algorithm and the original haze image. The largest CR values are also obtained by the URSHR algorithm and the smallest values are got by the DCP algorithm. The maximum values are almost 50 times of the minimum value (between Fig. 15(B)(a) and Fig. 15(B)(e)), indicating that the details obtained by the URSHR algorithm have a strong level sense. At the same time, the SSIM values of the URSHR algorithm are the smallest, which are 0.34 (Fig. 15(A)(e)) and 0.18 (Fig. 15(B)(e)), respectively, indicating that it has a strong ability to remove haze and to hold structure. After the above analysis, it can be concluded that the URSHR algorithm can also process some outdoor haze images, but the processing results of the far scene part are relatively poor. The MSMHC algorithm can obtain better results, which is shown in Fig. 15(d) and Table 4.

### G. EXPERIMENTS OF REMOTE SENSING IMAGE OF NATURAL SCENE

The following analysis is non-urban area remote sensing image, that is, the scene area covered by the image is mainly the natural landscape or countryside. The experimental data and results were shown in Fig. 16. The original remote sensing image data of the experiment is shown in from Fig. 16(A) to Fig. 16(D). They came from the QuickBird satellite and their resolution was 2.5m. The size of them is $660 \times 454$, $800 \times 600$, $600 \times 542$ and $800 \times 600$, respectively. Fig. 16(D) is a gray image, and other three are color images. These experimental images in Fig. 16 do not any contain artificial buildings. The experimental methods are still the DCP, BPDFHE, HE, MSMHC and URSHR algorithms, and the corresponding experimental results were shown in from Fig. 16(a) to Fig. 16(e), respectively. It can be seen in Fig. 16(e) that the URSHR algorithm can remove haze well and get a very good visual effect. It shows that the URSHR algorithm can also deal with the haze in non-urban remote sensing images. The results and laws of other methods are the same as those of the previous experiments. Although they are not as strong as the URSHR method in haze removal, they can also remove some haze and have
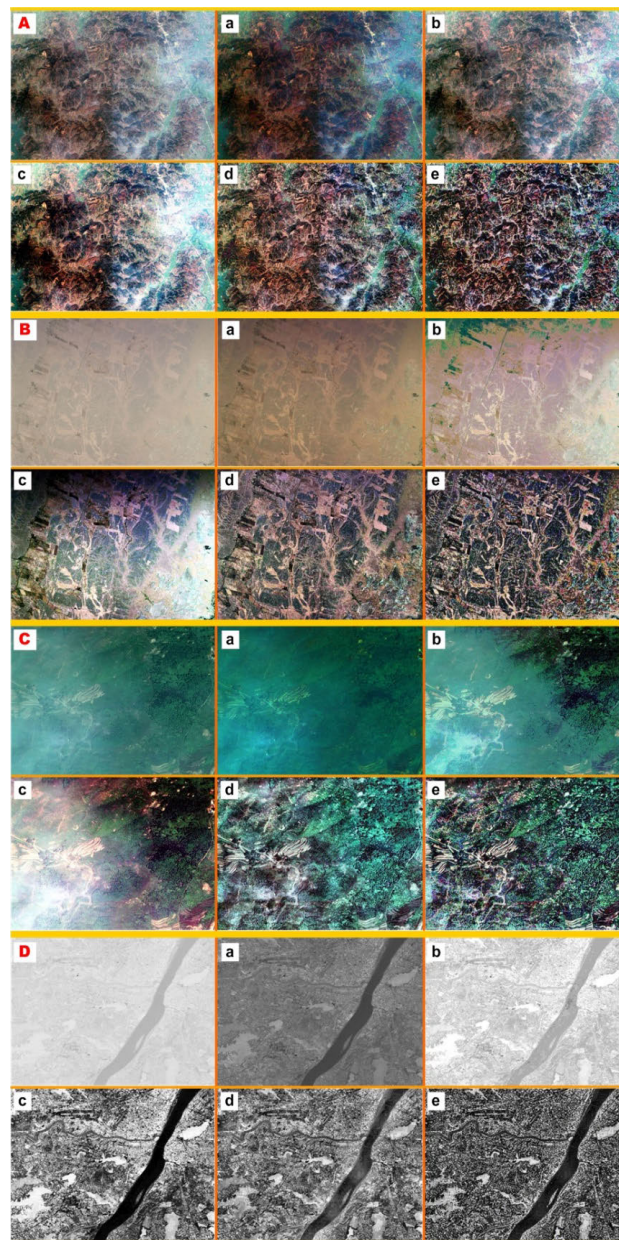


**FIGURE 16.** Experimental results of non-urban remote sensing haze images. A-D are the original non-urban remote sensing haze image, and a-e represents the experimental results obtained by DCP, BPDFHE, HE, MSMHC and URSHR method, respectively.

good interpretation ability, like the MSMHC method. It is seen in Fig. 16(d) that the effect of the MSMHC algorithm is also good. After comparing and analyzing the results shown in Fig. 16, it seems that the MSMHC algorithm is slightly better than the URSHR algorithm in terms of vision and details. The reason is that these images are natural landscape remote sensing images, which contain very rich and intricate details. When the URSHR algorithm removes haze, it will get over much detailed information. This will affect the correct interpretation, classification and recognition. Especially when the natural landscape is a large area forest and a sea

of great waves, the subsequent interpretation is more difficult, due to excessive details and intricate details. Therefore, the processing of haze in non-urban remote sensing image is not the advantage of the URSHR algorithm.

Through the comparison and analysis of the above series of experiments, it fully shows that each method has its advantages and disadvantages. In practical applications, we should choose appropriate methods according to the actual needs, processing purposes and image content. In a word, the URSHR algorithm can achieve good results for the haze removal of urban remote sensing image. It can not only process different types of remote sensing images and different resolution remote sensing images, but also can remove haze and get high definition and high contrast images. For other non-urban remote sensing images and outdoor images, URSHR algorithm can also process and remove haze, but it is not its main purpose and function.

## V. CONCLUSION

Haze is a kind of bad weather phenomenon in winter, which affects the image quality and target tracking of optical equipment. Due to the expansion and centralization of modern cities, haze has a more serious impact on urban remote sensing. Aiming at the problem of haze filtering in urban remote sensing image, this paper makes an in-depth discussion. After studying the characteristics of remote sensing image and the advantages, disadvantages and limitations of existing haze removal algorithms, according to the purpose and characteristics of urban remote sensing, a new algorithm of haze removal based on image phase consistency was proposed in this paper. Using different remote sensing images to verify the experiments, we can get better experimental results, and use the relevant parameters for quantitative evaluation. Experimental results fully prove that the URSHR algorithm proposed in this paper can get better detail information and high contrast, and has a strong ability to remove haze. Whether it is a low-resolution or high-resolution urban remote sensing image, whether it is a panchromatic or single band image, whether it is a synthetic multispectral color image or RGB image, it can achieve the desired effect. A series of experimental results show that the URSHR algorithm is a feasible and effective method to remove haze from urban remote sensing images.

## REFERENCES

[1] D. J. Jobson, Z. Rahman, and G. A. Woodell, "A multiscale retinex for bridging the gap between color images and the human observation of scenes," *IEEE Trans. Image Process.*, vol. 6, no. 7, pp. 965–976, Jul. 1997.

[2] X. Fu, Y. Sun, M. LiWang, Y. Huang, X.-P. Zhang, and X. Ding, "A novel retinex based approach for image enhancement with illumination adjustment," in *Proc. IEEE Int. Conf. Acoust., Speech Signal Process. (ICASSP)*, May 2014, pp. 1190–1194.

[3] K. He, J. Sun, and X. Tang, "Single image haze removal using dark channel prior," *IEEE Trans. Pattern Anal. Mach. Intell.*, vol. 33, no. 12, pp. 2341–2353, Dec. 2011.

[4] D. Singh and V. Kumar, "Dehazing of remote sensing images using improved restoration model based dark channel prior," *Imag. Sci. J.*, vol. 65, no. 5, pp. 282–292, Jul. 2017.

[5] R. T. Tan, "Visibility in bad weather from a single image," in *Proc. IEEE Conf. Comput. Vis. Pattern Recognit.*, Jun. 2008, pp. 1–8.

[6] R. Fattal, "Single image dehazing," *ACM Trans. Graph.*, vol. 27, no. 3, pp. 1–9, 2008.

[7] H. Ibrahim and N. P. Kong, "Brightness preserving dynamic histogram equalization for image contrast enhancement," *IEEE Trans. Consum. Electron.*, vol. 53, no. 4, pp. 1752–1758, Nov. 2007.

[8] D. Sheet, H. Garud, A. Suveer, M. Mahadevappa, and J. Chatterjee, "Brightness preserving dynamic fuzzy histogram equalization," *IEEE Trans. Consum. Electron.*, vol. 56, no. 4, pp. 2475–2480, Nov. 2010.

[9] S. Huang, D. Li, W. Zhao, and Y. Liu, "Haze removal algorithm for optical remote sensing image based on multi-scale model and histogram characteristic," *IEEE Access*, vol. 7, pp. 104179–104196, 2019.

[10] X. Yang, H. Li, Y.-L. Fan, and R. Chen, "Single image haze removal via region detection network," *IEEE Trans. Multimedia*, vol. 21, no. 10, pp. 2545–2560, Oct. 2019.

[11] J.-Y. Kim, L.-S. Kim, and S.-H. Hwang, "An advanced contrast enhancement using partially overlapped sub-block histogram equalization," *IEEE Trans. Circuits Syst. Video Technol.*, vol. 11, no. 4, pp. 475–484, Apr. 2001.

[12] A. K. Tripathi and S. Mukhopadhyay, "Single image fog removal using bilateral filter," in *Proc. IEEE Int. Conf. Signal Process., Comput. Control*, Piscataway, NJ, USA, Mar. 2012, pp. 1–6.

[13] W. Wang, W. Li, Q. Guan, and M. Qi, "Multiscale single image dehazing based on adaptive wavelet fusion," *Math. Problems Eng.*, vol. 2015, Oct. 2015, Art. no. 131082.

[14] C. O. Ancuti and C. Ancuti, "Single image dehazing by multi-scale fusion," *IEEE Trans. Image Process.*, vol. 22, no. 8, pp. 3271–3282, Aug. 2013.

[15] B. Cai, X. Xu, K. Jia, C. Qing, and D. Tao, "DehazeNet: An end-to-end system for single image haze removal," *IEEE Trans. Image Process.*, vol. 25, no. 11, pp. 5187–5198, Nov. 2016.

[16] Y. Song, J. Li, X. Wang, and X. Chen, "Single image dehazing using ranking convolutional neural network," *IEEE Trans. Multimedia*, vol. 20, no. 6, pp. 1548–1560, Jun. 2018.

[17] W. Ren, S. Liu, H. Zhang, J. Pan, X. Cao, and M.-H. Yang, "Single image dehazing via multi-scale convolutional neural networks," in *Proc. Eur. Conf. Comput. Vis.* Cham, Switzerland: Springer, 2016, pp. 154–169.

[18] W. Ren, J. Pan, H. Zhang, X. Cao, and M.-H. Yang, "Single image dehazing via multi-scale convolutional neural networks with holistic edges," *Int. J. Comput. Vis.*, vol. 128, no. 1, pp. 240–259, Jan. 2020.

[19] L.-F. Shi, B.-H. Chen, S.-C. Huang, A. O. Larin, O. S. Seredin, A. V. Kopylov, and S.-Y. Kuo, "Removing haze particles from single image via exponential inference with support vector data description," *IEEE Trans. Multimedia*, vol. 20, no. 9, pp. 2503–2512, Sep. 2018.

[20] Z. Xu, X. Liu, and X. Chen, "Fog removal from video sequences using contrast limited adaptive histogram equalization," in *Proc. Int. Conf. Comput. Intell. Softw. Eng.*, Dec. 2009, pp. 1–4.

[21] Y.-T. Kim, "Contrast enhancement using brightness preserving bi-histogram equalization," *IEEE Trans. Consum. Electron.*, vol. 43, no. 1, pp. 1–8, 1997.

[22] M. Abdullah-Al-Wadud, M. H. Kabir, M. A. A. Dewan, and O. Chae, "A dynamic histogram equalization for image contrast enhancement," *IEEE Trans. Consum. Electron.*, vol. 53, no. 2, pp. 593–600, May 2007.

[23] E. H. Land and J. J. McCann, "Lightness and retinex theory," *J. Opt. Soc. Amer.*, vol. 61, no. 1, pp. 1–11, 1971.

[24] E. H. Land, "The retinex theory of color vision," *Sci. Amer.*, vol. 237, no. 6, pp. 108–128, Dec. 1977.

[25] E. H. Land, "An alternative technique for the computation of the designator in the retinex theory of color vision," *Proc. Nat. Acad. Sci. USA*, vol. 83, no. 10, pp. 3078–3080, May 1986.

[26] D. J. Jobson, Z. Rahman, and G. A. Woodell, "Retinex image processing: Improved fidelity to direct visual observation," in *Proc. Color Imag. Conf.*, 1996, pp. 36–41.

[27] D. J. Jobson, Z. Rahman, and G. A. Woodell, "Properties and performance of a center/surround retinex," *IEEE Trans. Image Process.*, vol. 6, no. 3, pp. 451–462, Mar. 1997.

[28] Z. Rahman, D. J. Jobson, and G. A. Woodell, "Multi-scale retinex for color image enhancement," *IEEE Trans. Image Process.*, vol. 6, no. 7, pp. 1003–1006, 1996.

[29] K. Barnard and B. Funt, "Analysis and improvement of multi-scale retinex," in *Proc. Color Imag. Conf.*, 1997, pp. 221–226.

[30] K. He, J. Sun, and X. Tang, "Guided image filtering," *IEEE Trans. Pattern Anal. Mach. Intell.*, vol. 35, no. 6, pp. 1397–1409, Jun. 2013.

[31] Q. Zhu, J. Mai, and L. Shao, "A fast single image haze removal algorithm using color attenuation prior," *IEEE Trans. Image Process.*, vol. 24, no. 11, pp. 3522–3533, Nov. 2015.

[32] G. Wang, G. Ren, L. Jiang, and T. Quan, "Single image dehazing algorithm based on sky region segmentation," *Inf. Technol. J.*, vol. 12, no. 6, pp. 1168–1175, Jun. 2013.

[33] D. Singh and V. Kumar, "Single image haze removal using integrated dark and bright channel prior," *Mod. Phys. Lett. B*, vol. 32, no. 4, Feb. 2018, Art. no. 1850051.

[34] S. D. Thepade, P. Mishra, R. Udgirkar, S. Singh, and P. Mengwade, "Improved haze removal method using proportionate fusion of color attenuation prior and edge preserving," in *Proc. 4th Int. Conf. Comput. Commun. Control Automat. (ICCUBEA)*, Aug. 2018, pp. 1–5.

[35] J. Zhang, F. He, and Y. Chen, "A new haze removal approach for sky/river alike scenes based on external and internal clues," *Multimedia Tools Appl.*, vol. 79, pp. 2085–2107, Nov. 2019.

[36] A. Galdran, "Image dehazing by artificial multiple-exposure image fusion," *Signal Process.*, vol. 149, pp. 135–147, Aug. 2018.

[37] C. H. Chen, Y Liu, and Q. Cui, "Remote sensing image defog algorithm based on saturation operation and dark channel theory," *Comput. Eng. Appl.*, vol. 54, no. 5, pp. 174–179, 2018.

[38] C. L. Zhao and J. W. Dong, "Image enhancement algorithm of haze weather based on dark channel and multi-scale retinex," *Laser J.*, vol. 39, no. 1, pp. 104–109, 2018.

[39] Y. Li, Q. Miao, R. Liu, J. Song, Y. Quan, and Y. Huang, "A multi-scale fusion scheme based on haze-relevant features for single image dehazing," *Neurocomputing*, vol. 283, pp. 73–86, Mar. 2018.

[40] X. Zhao, K. Wang, Y. Li, and J. Li, "Deep fully convolutional regression networks for single image haze removal," in *Proc. IEEE Vis. Commun. Image Process. (VCIP)*, Dec. 2017, pp. 1–4.

[41] L. He, J. Bai, and M. Yang, "Feature aggregation convolution network for haze removal," in *Proc. IEEE Int. Conf. Image Process. (ICIP)*, Sep. 2019, pp. 2806–2810.

[42] L. Ke, P. Liao, X. Zhang, G. Chen, K. Zhu, Q. Wang, and X. Tan, "Haze removal from a single remote sensing image based on a fully convolutional neural network," *J. Appl. Remote Sens.*, vol. 13, no. 3, 2019, Art. no. 036505.

[43] K. Tang, J. Yang, and J. Wang, "Investigating haze-relevant features in a learning framework for image dehazing," in *Proc. IEEE Conf. Comput. Vis. Pattern Recognit.*, Jun. 2014, pp. 2995–3002.

[44] A. Makarau, R. Richter, R. Muller, and P. Reinartz, "Haze detection and removal in remotely sensed multispectral imagery," *IEEE Trans. Geosci. Remote Sens.*, vol. 52, no. 9, pp. 5895–5905, Sep. 2014.

[45] Q. Liu, X. Gao, L. He, and W. Lu, "Haze removal for a single visible remote sensing image," *Signal Process.*, vol. 137, pp. 33–43, Aug. 2017.

[46] M. C. Morrone and R. A. Owens, "Feature detection from local energy," *Pattern Recognit. Lett.*, vol. 6, no. 5, pp. 303–313, Dec. 1987.

[47] M. Chen, Q. Zhu, J. Zhu, Z. Xu, and L. Huang, "Interest point detection for multispectral remote sensing image using phase congruency in illumination space," *Acta Geodaetica Cartographica Sinica*, vol. 45, no. 2, pp. 178–185, 2016.

[48] Y. Lin, X. Fu, F. Wang, and H. You, "An oil spill segmentation algorithm for SAR imagery based on phase congruency," *Sci. Surv. Mapping*, vol. 41, no. 3, pp. 91–95, 2016.

[49] J. Kuang, Y. S. Zhang, and J. B. Zhao, "Automatic detection of rock mass fissure based on image processing of phase congruency," *Comput. Eng. Appl.*, vol. 54, no. 24, pp. 193–197, 2018.

[50] J. Long, Z. Shi, W. Tang, and C. Zhang, "Single remote sensing image dehazing," *IEEE Geosci. Remote Sens. Lett.*, vol. 11, no. 1, pp. 59–63, Jan. 2014.

[51] X. Pan, F. Xie, Z. Jiang, and J. Yin, "Haze removal for a single remote sensing image based on deformed haze imaging model," *IEEE Signal Process. Lett.*, vol. 22, no. 10, pp. 1806–1810, Oct. 2015.

[52] P. Kovesi, "Image features from phase congruency," *J. Comput. Vis. Res.*, vol. 1, no. 3, pp. 1–26, 1999.

[53] P. Kovesi, "Phase congruency detects corners and edges," in *Proc. 7th Int. Conf. Digit. Image Comput., Techn. Appl. (DICTA)*, 2003, pp. 309–318.

[54] Z. Ahmed, M. Sayadi, and F. Faniech, "Satellite images features extraction using phase congruency model," *Int. J. Comput. Sci. Netw. Secur.*, vol. 9, no. 2, pp. 192–197, 2009.

[55] E. J. McCartney, *Optics of the Atmosphere: Scattering By Molecules and Particles*. New York, NY, USA: Wiley, 1976.

**SHIQI HUANG** (Member, IEEE) received the B.S. degree from the Department of Information Management, Chinese Agriculture University (CAU), Beijing, China, in 1998, and the M.S. and Ph.D. degrees from the Xi'an Research Institute of Hi-Tech, Xi'an, China, in 2004 and 2008, respectively.

He is currently a Professor with the School of Automation, and a Graduate Teacher with the Xi'an University of Posts and Telecommunications, Xi'an. He has published three academic monographs and published more than 100 academic articles. His main research interests include target detection and recognition, change information obtaining and processing, remote sensing image processing and applications, and big data processing and application. He is a Council Member of the Shaanxi Provincial Society of Graphic Imaging and the Shaanxi Provincial Geophysical Society, China.

**YANG LIU** received the B.S. degree from the Department of Exploration Technology and Engineering, Yangtze University, Jingzhou, Hubei, China, in 2010, and the M.S. and Ph.D. degrees from the China University of Petroleum, Beijing, China, in 2012 and 2015, respectively.

She is currently a Teacher with the School of Automation, Xi'an University of Posts and Telecommunications, Xi'an, China. Her main research interests include image signal processing and analysis, artificial intelligence, and optimal algorithms.

**YITING WANG** received the B.S. degree in signal processing from the Cheng Du University of Information Technology, in 2010, and the M.S. and Ph.D. degrees in information and communication engineering from the Rocket Force University of Engineering, Xi'an, Shaanxi, China, in 2013 and 2017, respectively.

She is currently a Lecturer with the Rocket Force University of Engineering. Her research interests include hyperspectral image processing and application, deep learning, quantitative remote sensing, and so on.

**ZULIANG WANG** was born in Yunan, China. He received the M.S. and Ph.D. degrees in information and communication engineering from the National University of Defense Technology, Changsha, China, in 2004 and 2008, respectively. He is currently a Professor working with the School of Information Engineering, Xijing University, China. His scientific interests and experience are related to the radio frequency identification, anti-collision, and the Internet of Things. He is the author or coauthor of more than 40 scientific publications and 15 patents.

**JINKU GUO** received the M.S. and Ph.D. degrees from the Rocket Force University of Engineering, Xian, China, in 2005 and 2010, respectively.

He is currently an Associate Professor with the Unmanned System Research Institute, Northwestern Polytechnical University (NPU), Xi'an. He is also with postdoc innovation base on Xian Daheng Tian Cheng IT Company, Ltd. His main research interests include signal processing and analysis, artificial intelligence and optimal algorithms, electromagnetic and computer simulation, and image processing.

• • •